VIETNAM MEDICAL ASSOCIATION
VIETNAM ASSOCIATION OF PHYSIOLOGY

Vietnam Journal of PHYSIOLOGY

Tập 26, №3
9/2022

Vietnam Journal of Physiology
Volume 26, №3, September 2022

VIETNAM JOURNAL OF PHYSIOLOGY

Editorial Office

First Floor, B3 Building, Hanoi Medical University
No1 Ton That Tung Street, Dong Da District, Hanoi City
Tel: 84-438523798. Ext: 203, 205, 207 Email: tapchi@sinhlyhoc.com.vn

Contact Addresses

1. Vu Thi Thu PhD.
Dept. of Human Bio. and Phy., Falcuty of Physiology, VNU University of Science
No334 Nguyen Trai Street, Thanh Xuan District, Hanoi City, VN
Cell phone: 0903 237 808 Email: tapchi@sinhlyhoc.com.vn

THỂ LỆ GỬI BÀI ĐĂNG TẠP CHÍ SINH LÝ HỌC VIỆT NAM

Tạp chí Sinh lý học Việt Nam là tạp chí chuyên ngành Sinh lý học. Tạp chí đăng tải các công trình nghiên cứu, các bài tổng quan, thông báo khoa học thuộc chuyên ngành Sinh lý học và các chuyên ngành có liên quan với Sinh lý học Y học, Sinh lý học Người và Động vật.

1. Quy định chung về bài đăng trên Tạp chí Sinh lý học Việt Nam

- Các thuật ngữ thống nhất theo tự điển Bách khoa Việt Nam.
- Bài gửi đăng phải đánh máy bằng tiếng Việt rõ ràng, phông chữ Unicode, kiểu chữ Arial, cỡ chữ 10, khổ giấy 26.5*19.0 cm, lề trên 2cm, lề dưới 2cm, lề trái 2.5cm, lề phải 2.5cm, cách dòng 1.15 line. Các chữ viết tắt phải được chú thích các từ gốc của các chữ viết tắt đó. Thứ tự các đề mục đánh số Ả-rập, không đánh số La Mã (Thí dụ 1, 1.1, 1.1.1, 2, 2.2...).
- Bài đăng Tạp chí gửi về địa chỉ **https://tapchi.sinhlyhoc.com.vn/index.php/vjp/index**, gửi kèm theo tên, địa chỉ liên lạc, địa chỉ email và số điện thoại của tác giả chịu trách nhiệm khoa học về bài báo (Tạp chí không nhận bản in).
- Mỗi tác giả được phép đăng nhiều bài trong 1 số nhưng chỉ được đứng tên đầu ở 1 bài. Bài không đăng được, không trả lại bản thảo.
- Tác giả chịu trách nhiệm khoa học của bài báo phải ký vào văn bản cam kết về bản quyền của mình, các số liệu nghiên cứu, nội dung được đưa ra trong bài báo, các vấn đề về đạo đức nghiên cứu và gửi về địa chỉ Ban biên tập:

Văn phòng Hội Sinh lý học Việt Nam
Tầng 1, Nhà B2, Trường Đại học Y Hà Nội,
Số 1, Phố Tôn Thất Tùng, Quận Đống Đa, TP Hà Nội

2. Một số yêu cầu cụ thể về bài đăng công trình nghiên cứu khoa học

- Bài gửi đăng chưa được đăng ở bất kỳ Tạp chí quốc gia nào.
- Tổng số trang của bài đăng công trình không quá 8 trang giấy A4, không quá 10 trang với bài tổng quan.
- Tổng số các đối tượng minh họa, kết quả (gồm hình, bảng, biểu) không quá 5 (gồm bảng, biểu, hình, ảnh, biểu đồ) và/hoặc 1/4 tổng số trang của bài báo. Tên các đối tượng được ghi theo số thứ tự cho mỗi loại (ví dụ hình 1, hình 2, bảng 1, bảng 2). Tên bảng được đặt ở trên, chính giữa bảng, tên hình, biểu đồ được đặt ở dưới, chính giữa hình, biểu đồ.
- Lệ phí đăng bài là 600.000 đồng/bài và 200.000 chi phí in ấn/bài. Kinh phí được thu nộp khi bài báo được chấp nhận đăng. Thông tin tài khoản của Hội Sinh lý học Việt Nam như sau:

Đoàn Thị Vân Du
Số tài khoản: **1221 0001 39 0003.**
tại Ngân hàng BIDV chi nhánh Hà Thành

- Trình tự các mục trong bài:
  + Tên bài báo: Được viết ngắn gọn, thể hiện được nội dung chính của bài báo và bắt đầu bằng danh từ
  + Họ và tên các tác giả, địa chỉ cơ quan, nơi thực hiện công trình (không ghi học hàm, học vị, chức danh). Tác giả thực hiện chính được viết đầu tiên, tác giả chịu trách nhiệm khoa học về bài báo được viết cuối cùng nếu có (ví dụ tên thầy hướng dẫn). Cuối trang thứ nhất của bài báo cần ghi rõ tên tác giả chịu trách nhiệm khoa học về bài báo, kèm theo địa chỉ liên lạc, địa chỉ email và số điện thoại. Liệt kê đầy đủ tất cả các tác giả tham gia bài báo, đề nghị không viết "và cộng sự".
  + Tóm tắt tiếng Việt: Viết không quá 300 từ, viết dưới dạng bài văn xuôi thể hiện được mục tiêu, đối tượng nghiên cứu, phương pháp nghiên cứu, kết quả chính của nghiên cứu và kết luận. Từ khóa không quá 5 từ, cụm từ.
  + Tên bài báo và tóm tắt bằng tiếng Anh đặt ở cuối bài báo, sau tài liệu tham khảo, cần được dịch đầy đủ chính xác từ tên bài báo, tóm tắt và từ khóa bằng tiếng Việt.
  + Nội dung toàn văn gồm:

- √ Đặt vấn đề (bao gồm cả mục tiêu nghiên cứu của đề tài): Cần nêu rõ lý do hoặc giả thuyết nghiên cứu, mục tiêu nghiên cứu (không trùng lặp với tên bài báo).
- √ Đối tượng và phương pháp nghiên cứu: Viết ngắn gọn, đầy đủ thông tin bao gồm: đối tượng nghiên cứu, thiết kế nghiên cứu, công cụ nghiên cứu, phương pháp thu thập số liệu, phương pháp phân tích số liệu, đạo đức nghiên cứu.
- √ Kết quả nghiên cứu: được thể hiện bằng các bảng, biểu đồ, hình hoặc bằng lời.
- √ Bàn luận (bàn luận có thể viết chung với kết quả nghiên cứu, trong trường hợp viết chung thì đề mục cần ghi rõ "Kết quả và bàn luận"): tác giả cần so sánh kết quả nghiên cứu của mình với các tác giả khác và lý giải về kết quả thu được.
- √ Kết luận: viết ngắn gọn, trả lời đầy đủ mục tiêu đề ra.
- √ Khuyến nghị: nếu có.
- √ Lời cảm ơn: cảm ơn quỹ tài trợ, nơi thực hiện nghiên cứu, các cộng sự đóng góp cho công trình.
- √ Tài liệu tham khảo

3. Quy định về tài liệu tham khảo

- Tài liệu tham khảo (không quá 15 tài liệu) được xếp theo thứ tự vần chữ cái A, B, C..., tiếng Việt trước, tiếng nước ngoài sau.
- Nếu tài liệu là tạp chí thì ghi tên tác giả, năm xuất bản, tên bài, tên tạp chí, tập, số, trang (đầu và cuối). Ví dụ:
  + **Dean P, Michell IJ, Redgrave P (1988),** Responses resembling defensive behaviour produced by microinjection of glutamate into superior colliculus of rats. Neuroscience, 24(2):501-510.
- Trường hợp tài liệu tham khảo có từ **3** tác giả trở xuống thì ghi đầy đủ họ tên của 10 tác giả. Trong trường hợp có từ **3** tác giả trở lên thì ghi đầy đủ họ, tên của 3 tác giả đầu tiên, sau đó viết "và cộng sự" nếu bài báo viết bằng tiếng Việt hoặc "et al" nếu bài báo viết bằng tiếng nước ngoài. Ví dụ:
  + **Dommett E, Coizet V, Blaha CD, et al (2005),** How visual stimuli activate dopaminergic neurons at short latency. Science, 307(5714):1476-1479.
- Nếu là sách chuyên khảo thì ghi tên tác giả, năm xuất bản, tên sách, nhà xuất bản, TP xuất bản, trang tham khảo. Ví dụ:
  + **Stein BE, Meredith MA (1993),** The merging of the senses. Cambridge, MA: MIT, pp.230-235.
- Nếu là một chương trong sách thì ghi tên tác giả của chương, năm xuất bản, tên chương, tên sách, tên người biên tập, thành phố xuất bản, nhà xuất bản, trang tham khảo. Ví dụ:
  + **Gerfen CR, Wilson CJ (1996),** The basal ganglia. In: Handbook of chemical neuroanatomy, Vol 12: Integrated systems of the CNS, Part III. (Swanson LW, Bjorklund A, Hokfelt T, eds), Amsterdam: Elservier, pp.371 - 468.
- Nếu tài liệu không thuộc hệ chữ Latinh thì phiên âm tên tác giả (theo tiếng Latinh) và dịch toàn bộ phần còn lại ra tiếng Việt, sau đó mở ngoặc ghi chú tiếng của tài liệu đó. Ví dụ: (tiếng Nga).
- Các tài liệu đưa ra phải được trích dẫn đầy đủ trong nội dung bài báo. Trong đó ít nhất 50% số tài liệu tham khảo cần xuất hiện trong phần bàn luận.

4. Yêu cầu đối với các bài tổng quan, thông báo khoa học và bài dịch

- Đối với các bài Tổng quan cần có đầy đủ các tài liệu tham khảo và nguồn số liệu được trích dẫn trong bài. Tác giả bài Tổng quan được ghi rõ chức danh khoa học, học vị, chuyên ngành, địa chỉ cơ quan (ghi ở cuối trang đầu của bài Tổng quan). Nếu bài tổng quan dài, Ban biên tập sẽ chia làm 2 kỳ, mỗi kỳ dài không quá 10 trang, kể cả hình ảnh, bảng, biểu và tài liệu tham khảo. Số tài liệu tham khảo không quá 20 tài liệu.
- Đối với các bài Thông tin khoa học, các bài dịch cần ghi rõ xuất xứ của nguồn dữ liệu được sử dụng để viết bài thông tin hoặc bài dịch. Đối với bài dịch cần photocopy toàn văn bản bài báo tiếng nước ngoài gửi kèm theo bản dịch.
- Đối với bài tổng quan và các bài thông tin khoa học, tác giả gửi đăng sẽ không phải nộp lệ phí khoa học.

TABLE OF CONTENT

This journal is published under the approval of Ministry of Information and Communications, No. 312/GP-BVHTT dated 23/7/2002. Copyright deposit in September, 2022

STABILITY OF THE TRANSGENE REPORTER FOR OSTEOBLASTS IN THE TRANSGENIC *COL10A1*:NLGFP MEDAKA FISH (*ORYZIAS LATIPES)*

To Thanh Thuy[1], Nguyen Thi Thu Ha[1], Nguyen Tuong Anh[1], Ha Thi Minh Tam[1], Nguyen Huy Manh[1],Tran Thi Thuy Chinh[1], Tran Duc Long[1]

SUMMARY

Objective: *to examine genetic and functional stability of an osteoblast reporter transgene coding for green fluorescence protein (GFP) in the transgenic col10a1:nlGFP fish generated a decade ago.* ***Methods:*** *homozygous and hemizygous fish for the transgene GFP were segregated by testcrossing. PCR were performed to check for the presence of the transgene GFP in the homozygous and hemizygous genomes. GFP signal was used to assess distribution of collagen10a1 expressing osteoblasts. Alizarin complexone (ALC) was used to visualize mineralized matrix of the live larvae. Expression pattern of the transgene GFP and level of bone mineralization in the live transgenic fish was analyzed using fluorescent imaging and ImageJ analysis for GFP and ALC signal, respectively.* ***Results:*** *three homozygous col10a1:nlGFP fish were found and many hemizygotes were produced. Both homozygous and hemizygous fish still contain the transgene GFP in their genomes and express GFP in a pattern recapitulating endogenous collagen10a1 gene expression in osteoblast. They also retain the pattern of GFP expression in bone structures like that of the original transgenic fish generated a decade ago. This confirms the genomic and functional stability of the transgene GFP in the fish.*

Key words: *medaka, transgenics, col10a1, osteoblasts, GFP.*

1. INTRODUCTION

Medaka fish (*Oryzias latipes) have* been increasingly used as a preferable model organism to study biological processes and human diseases including bone diseases [1–3]. Sharing high similarity in genome and in basic biological processes to humans [1, 4, 5], medaka fish own numerous experimental advantages that out compete and complement to mammalian models including low cost for maintenance, short generation time, external embryogenesis, large amount of small and transparent embryos [2, 3]. These features facilitate fish transgenesis and mutagenesis [6–8]. Transgenesis enables marking cells of interest by fluorescence proteins, promoting observation of live cells which are being in differentiation, in cell-cell interaction and in activity, both in healthy and diseased conditions [9–12].

Bone is a dynamic tissue whose health depends largely on balance between bone resorption by osteoclasts, bone ”eating” cells, and bone formation by osteoblasts, bone forming cells. Molecular network controlling these two processes as well as interaction between these two types of bone cells are very important for understanding mechanism underlying bone health and bone disorders. Thus, animal models that can allow observation of bone cells are important tools for bone studies and medaka fish is a good organism for this purpose.

Different transgenic medaka fish have been generated and used as tools to show high similarity in bone metabolism processes to humans at the cellular and

[1]Faculty of Biology, University of Science Vietnam National University
Corresponding author: **To thanh Thuy**
Email: tothanhthuy@hus.edu.vn
Received date: 04/8/2022
Reviewed date: 01/9/2022
Accaepted date: 15/9/2022

molecular levels [9, 11, 13, 9]. The *col10a1*:nlGFP medaka fish expresses green fluorescent protein (GFP) in *collagen10a1 (col10a1)* expressing osteoblasts is one important osteoblast reporter line which can track or report osteoblasts by GFP signal. The fish was generated by insertion of a transgene construct containing a 5.865 kb promotor region of the medaka *col10a1* gene followed by GFP coding sequence and a nuclear localization signal (nlGFP) into the medaka genome using meganuclease transgenic technique [11]. In this fish, expression of nlGFP driven by *col10a1* promotor was shown to recapitulate endogenous *col10a1* expression. Transgenic embryos at 4 dpf showed first *nlGFP* expression in the head bone structures including the operculum, parasphenoid and cleithrum, where endogenous *col10a1* was also first found to be expressed in wild-type fish [14]. Using this *col10a1*:nlGFP transgenic fish, researchers were able to analyze the process of mineralization of medaka vertebral column and differentiation of different type of osteoblasts involved in the process [11].

The transgenic fish was gifted to us in 2012, a decade ago, and has since been maintained in our laboratory. As multiple unknown factors can affect function of transgenes in transgenic animals, the transgenic fish was tested for the genomic and functional stability of the transgene GFP. The transgenic fish was testcrossed to generate homozygotes and hemizygotes and the presence of the transgene GFP in the fish genome was examined. The expression pattern of the transgene GFP was analyzed in parallel with alizarin complexone signal for mineralized matrix.

2. MATERIALS AND METHODS

2.2. Fish lines and fish maintenance

For this study, *col10a1*:nlGFP and wild type fish were used. Fish were raised and maintained according to established procedures in an air-conditioned facility with temperature set at 28-30^{o}C and 14h light/10h dark cycles [15]. Fish embryos were raised in E3 medium as previously reported [9, 15]. All fish experiments were performed in accordance with the animal welfare laws and guidelines from Dinh Tien Hoang Institute of Medicine, Hanoi, Vietnam (Approval number: IRB-AR.002).

2.3. Homozygous fish screening using test cross

After several generations of random mating with wild type fish, fish expressing green fluorescence protein (screened using Zebrafish fluorescent observation kit, Lumos Technology Co. Ltd., Taiwan) can be homozygous or hemizygous for the *col10a1*:nlGFP transgene. These fish were then test-crossed with wild-type fish to obtain embryos. If 100% of the embryos express GFP, their transgenic father/mother is a homozygote. Thereafter, parent fish were separated into tanks and raised to collect homozygous offsprings or crossed with wild-type fish to provide hemizygotes.

2.4. Live staining of mineralized matrix

For *in vivo* staining of calcified bone, embryos were dechorionated with hatching enzyme as described (Kinoshita et al., 2009). Dechorionated embryos were incubated in medium containing Alizarin Complexone (ALC, 0.02%) and subsequently washed in embryo medium. Calcification (Alizarin Complexone, ALC) and *col10a1*:nlGFP expression in embryos and larvae were analyzed with fluorescent microscopy (STEREO Discovery V8) using GFP and RFP filter settings. Images were captured at 8X magnification using BUC5F-2000C Microscope Digital Camera (Bestcope) and analyzed using ImageJ software.

2.5. DNA extraction and PCR amplification of GFP gene fragment

Homozygous and hemizygous embryos were collected along with the wild type and raised separately until 4 dpf.

Their DNAs were then extracted using a previously published protocol (ZFIN: Zebrafish Book: Molecular Methods). Next, extracted DNA was used for PCR amplification with primers eGFP.F1 CTGACCCTGAAGTTCATCTGC and eGFP.R1 GTCCATGCCGAGAGTGATCC. The expected PCR product was 579 bp and analyzed by agarose gel electrophoresis.

2.6. Statistical analyses

Due to optical limitations, an image captures only two to three vertebrae of an 11-day-old larva. Thus, four or five iamges were stitched together using ImageJ to fully show the whole body of the larva. Polygon selection tool was used to determine the Region of Interest (ROI) which covered five vertebral bodies and their neural arches. The mean gray value of five ROIs (from the 8th vertebrae to the 12th) was then calculated for each larva. Two-tailed Student's t-test was applied for comparison of fluorescent signal between the homozygous and hemizygous groups. The level of significance was set as follows: *0.01 < p < 0.05, **p < 0.01, ***p < 0.001 and ****p < 0.0001. Graphs were created using Graphpad Prism 8 software.

3. RESULTS

3.1. Segregation of the col10a1:nlGFP fish and generation of homozygous fish

The *col10a1*:nlGFP fish was generated in National University of Singapore [11]. This fish was gifted to us in 2012 and has since been raised and maintained in our laboratory. The original fish was outcrossed and testcrossed to generate homozygous and hemizygous lines for the transgene nlFGP. Original *col10a1* fish (F0 fish) were outcrossed with wild type (WT) fish to obtain F1 fish. F1 fish were testcrossed with WT fish and checked for Medelian segregation ratio of 1 GFP+: 1 GFP in F2 embryos to find heterozyous F1 fish with single insertion the transgene (data not shown). Hemizygous fish were maintained for many generations and inbred to obtain homozygous fish (F3 fish). Three homozygous fish were found after testcrossing 8 offsprings of hemizygous parents (Table 1).

Table 1: Screening for homozygous col10a1:nlGFP fish

F3 individual	GFP positive (F4 embryos)	GFP negative (F4 embryos)	GFP+:GFP- ratio	F3 fish homozygous or hemizygous
Col.m1	51	52	50% (1:1)	hemizygous
Col.m2	258	0	100% GFP+	**homozygous**
Col.f1	121	0	100% GFP+	**homozygous**
Col.f2	42	52	50% (1:1)	hemizygous
Col.f3	125	0	100% GFP+	**homozygous**
Col.m3	60	81	50% (1:1)	hemizygous
Col.m4	69	95	50% (1:1)	hemizygous
Col.m5	33	24	50% (1:1)	hemizygous
Col.m6	21	35	50% (1:1)	hemizygous

Name of individual fish was given as Col.(abbreviation of collagen10a1:nlGFP) followed by a "m" (male fish) or a " f" (female fish) letter and a number representing the fish.

The homozygous fish were inbred to generate a homozygous fish pool which presently has about 300 individuals.

3.2. Genetic stability of the transgene GFP in the genome of *col10a1*:nlGFP fish

Integrity of the transgene GFP reporter for osteoblasts in the genome of the *col1a1*:nlGFP fish was examined by PCR. DNA was extracted from hemizygous, homozygous, and wild-type larvae and used as template to amplify a 579 base pairs fragment of GFP coding sequence (Figure 1).

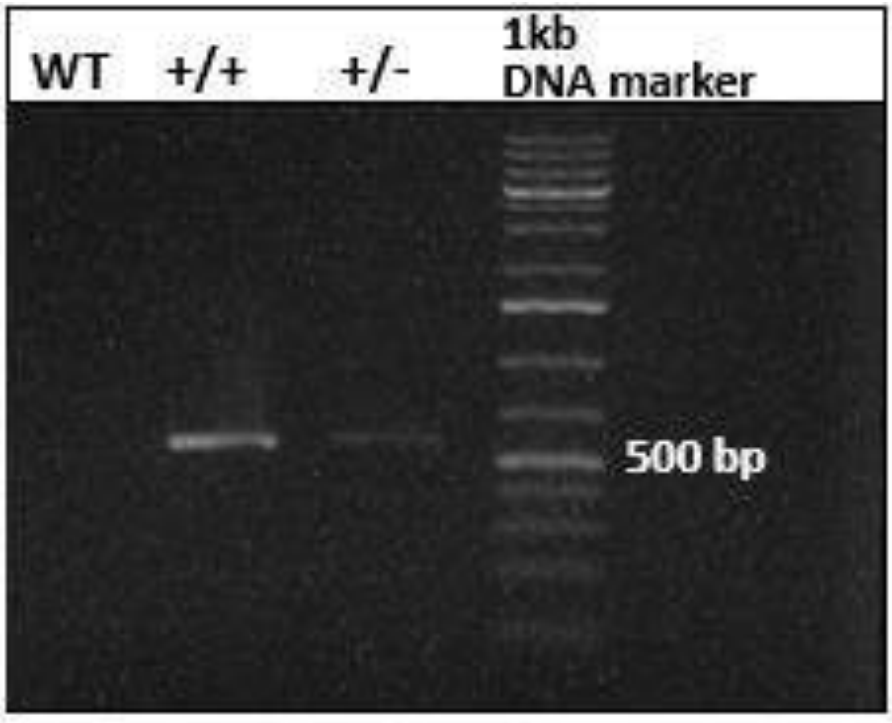

Figure 1: GFP coding sequence in the genome of *col10a1*:nlGFP fish.
PCR amplification of a 579 bp fragment of GFP coding sequence from genomic DNA extracted from wild-type (WT) homozygous (+/+) and hemizygous (+/-) col10a1:nlGFP fish embryos

A fragment of the expected size (of about 579 bp) was amplified from DNA of both hemizygous and homozygous fish, while wild-type DNA shows no band (Figure 1). Moreover, the intensity of the band is higher in homozygotes compared to that of hemizygous fish when similar amounts of DNA templates were used for PCR. This indicates that the transgene GFP is still presented in the genome of the transgenic fish, and the homozygotes carries two transgene alleles while the hemizygotes only one.

3.3 Expression patterns of GFP in homozygous and hemizygous *col10a1*:nlGFP recapitulate expression of endogenous *col10a1* gene and that of original transgenic fish.

GFP expression pattern in hemizygous (+/-) and homozygous (+/-) larvae were examined at 4, 6, 7, 10, and 14 dpf. In general, the GFP expression in both +/+ and +/- fish remain recapitulating endogenous *col10a1* gene expression (Figure 2, 3, and data not shown) as reported previously [11, 14]. This is evidenced by the first GFP expression observed in head skeleton including the operculum (op), parasphenoid (p), and cleithrum (cl) at 4dpf (Figure 2A', B), where endogenous expression of *col10a1* in wild type fish was also observed [14]. At 6 dpf, GFP signals are also observed in some anterior vertebrae, their neural arches (na), and in some fin rays (fr) (Figure 2C', E).

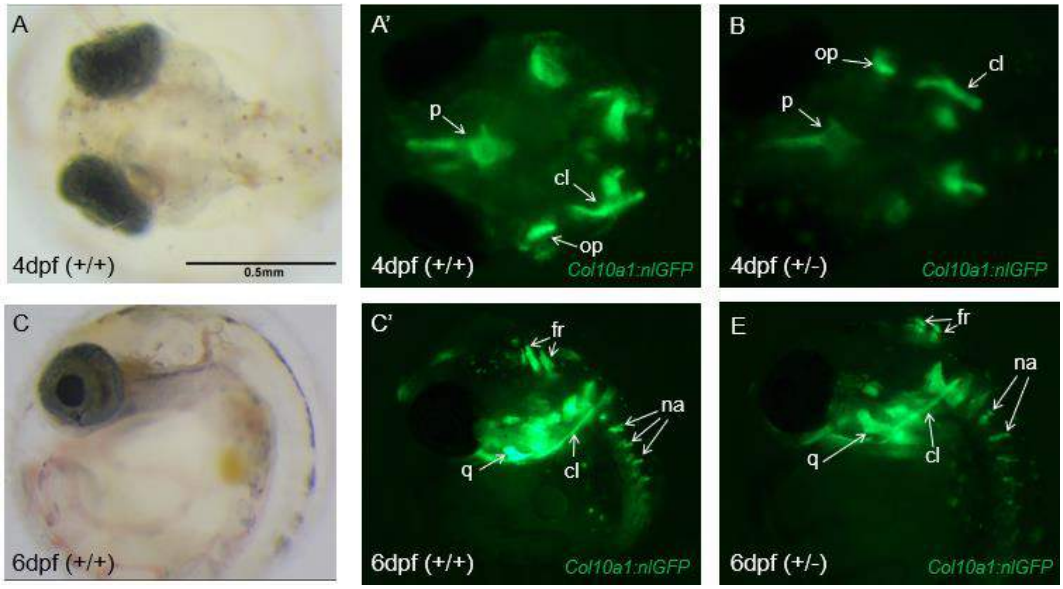

Figure 2. Expression pattern of *col10a1*:nlGFP in 4 dpf and 6 dpf homozygous (+/+) and hemizygous (+/-) larvae.

A and A': brightfield and fluorescent dorsal images of the head of a 4-day old homozygous larva. C and C': brightfield and fluorescent dorsal images of the head of a 6-day old homozygous larva. p: parasphenoid, cl: cleithrum, op: operculum, na: neural arches, q: quadrate, fr: fin rays.

GFP expression pattern of 10-day old homozygous and hemizygous larvae was also similar to that of original *col10a1*:nlGFP transgenic fish [11], as representatively indicated in Figure 3a.

3.4 ALC density is unchanged in hemizygous and homozygous *col10a1*:nlGFP fish

Figure 3a shows representative images of *col10a1*:nlGFP signal and alizarin complexone (ALC) stained homozygous (+/+) and hemizygous (+/-) live fish at 10dpf. Quantification of GFP and ALC signals of 5 representative vertebrae (boxed in B, B', E, E' are enlarged in C, C', F, F' of Figure 3a, respectively) of homozygous (+/+) and hemizygous (+/-) larvae (n = 7 for each group) results in Figure 3b. GFP signal intensity of homozygous fish is significantly higher than that of hemizygous fish (227.7 versus 114.2) while the values of ALC signal intensity are indifferentiable between these two groups (182.8 versus 173.0).

4. DISCUSSION

In this study, we have examined genomic and functional stability of the transgene GFP in homozygous and hemizygous col10a1:nlGFP fish. After a decade of maintenance in our laboratory, we have shown that the transgene is still integrated in the fish genomes and homozygous fish genomic DNA generated higher amplification of the transgene than that of hemizygous fish (Figure 1). We have further shown that, functionally, the GFP transgene, after a decade being integrated in the medaka fish genome, remains intact as its expression observed via GFP signal using fluorescent microscopy recapitulating endogenous col10a1 gene expression as previously reported [14] and reflecting expression pattern of col10a1:nlGFP in the original transgenic fish (Figure 2) [11]. Moreover, we showed that the intensity of col10a1:nlGFP signal in the homozygous fish is higher (almost two folds higher) than

that of the hemizygous fish (Figure 3b). This may be resulted from the expression of two alleles of the transgene GFP in the homozygous larva compared to that of one allele in hemizygous larva. Thus, it is important to segregate the fish into homozygous and hemizygous lines for the proper use that need individual larva with similar levels of GFP expression as indicator for number and activity of osteoblasts. Even though having higher intensity of GFP signal, homozygous fish have same intensity of ALC signal (Figure 3b) indicating GFP expression does not affect level of bone mineralization of the fish.

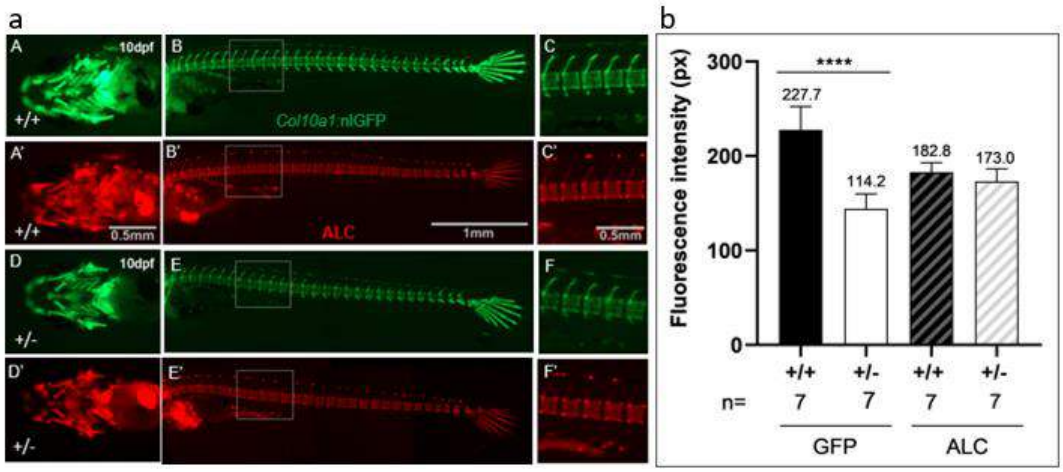

Figure 3. nlGFP expression and ALC bone mineralization signal in homozygous and hemizygous *col10a1*:nlGFP-fish larvae at 10dpf.

a. *A-C: images of col10a1:nlGFP signal in the head (A, ventral view), in the trunk and tail (B, lateral view) and in 5 representative vertebrae (boxed in B) of one homozygous (+/+) larva; A'-C': images of ALC signal of the same larva. D-F': similar demonstration as A-C' for one hemizygous (+/-) larva.*

b. *Statistical quantification of intensities of green (col10a1:nlGFP for osteoblasts) and red (ALC for mineralized bone matrix) fluorescent signals measured in 5 representative vertebrae (boxed in B, B', E, E' and enlarged as C, C', F, F, respectively) of the two fish; n: number of analysed fish in corresponding group. Two-tailed, unpaired t-test. Bars indicate S.E.M. ****p<0.001*

Understanding mechanisms controlling behaviors and activity of osteoblasts and osteoclasts and their interaction is the key to find out strategies for development of drugs and treatments for bone diseases. The *col10a1*:nlGFP fish expresses green fluorescent protein (GFP) in *collagen10a1* expressing osteoblasts is one important osteoblast reporter fish line because it allows tracking or reporting live and functional osteoblasts by GFP signal. Studies have shown that osteoblasts in medaka also undergo different stages of differentiation and each stage is represented by expression of certain specific genes, similar to that of humans [11, 13, 14]. Using this fish, researchers were able to analyze the process of mineralization of medaka vertebral column and differentiation of osteoblasts involved in the process [11]. *Col10a1*:nl GFP expression appeared in a segmental pattern before the ossification of the notochordal sheath [11]. With this fish, role of osteoblasts in bone healing from damage induced by Rankl was

investigated [11]. The use of this fish also help finding out factors important for osteoclasts differentiation and activity during bone resorption process induced by Rankl [12]. Recently this fish have used for assessment of bone protective effects of substances [15]. Thus, maintenance a stable transgenic *col10a1*:nlGFP fish is crucial for studying bone metabolism and bone diseases.

5. CONCLUSION

The *col10a1:*nlGFP transgene is genetically and functionally stable in both hemizygous and homozygous *col10a1*:nlGFP transgenic fish generated a decade ago. In these fish, *col10a1* expressing osteoblasts are marked by GFP signal and hence can be observed lively under fluorescent microscopes. This fish can be further used for studies on bone and bone diseases.

Acknowledgements

We thank Assoc. Prof. Nguyen Lai Thanh, Dr. Vu Thi Thu, and staffs of CELIFE, Faculty of Biology, VNU University of Science for assistance in microscopic imaging. This research was funded by the Vietnam National Foundation for Science and Technology Development (NAFOSTED) under the Grant number 106-YS.06-2014-15.

REFERENCES

1. **Witten PE, Harris MP, Huysseune A, et al (2017).** Small teleost fish provide new insights into human skeletal diseases, Methods Cell Biol., 138, pp. 321–346.
2. **Naruse K, Tanaka M, Takeda H (2011).** Medaka - A Model for Organogenesis, Human Disease, and Evolution, Science. 2011.pp. 132 p.
3. **Hiromi Hirata AI (2018).** zebrafish, medaka and other small fishes, new model animal in Biology, medicine and beyond, Hirata, Hiromi, Iida A, editor. 2018.
4. **Schartl M (2014),** Beyond the zebrafish: diverse fish species for modeling human disease, Dis. Model. Mech.,.
5. **Kettleborough RNW, Busch-Nentwich EM, Harvey SA, et al. (2013).** A systematic genome-wide analysis of zebrafish protein-coding gene function, Nature, 496, pp. 494–497.
6. **Soroldoni D, Hogan BM, Oates AC (2009).** Simple and efficient transgenesis with meganuclease constructs in zebrafish., Methods Mol. Biol., 546, pp. 117–130.
7. **Davidson AE, Balciunas D, Mohn D, et al. (2003).** Efficient gene delivery and gene expression in zebrafish using the Sleeping Beauty transposon, Dev. Biol., 263(2), pp. 191-202.
8. **G.H. Boon Ng, Z. Gong (2011),** Maize Ac/Ds transposon system leads to highly efficient germline transmission of transgenes in medaka (Oryzias latipes), Biochimie, 93(10), pp. 1858–1864.
9. **T.T. To, P. Eckhard Witten, J. Renn, D. Bhattacharya, A. Huysseune, C. Winkler (2012),** Rankl-induced osteoclastogenesis leads to loss of mineralization in a medaka osteoporosis model, 139(1), pp. 141–150.
10. **K. Inohaya, Y. Takano, A. Kudo (2007),** The teleost intervertebral region acts as a growth center of the centrum: In vivo visualization of osteoblasts and their progenitors in transgenic fish, Dev. Dyn.,.
11. **A. Büttner, T.T. To, C. Winkler, S.J.H. Chan, J. Renn (2013),** A col10a1_nlGFP transgenic line displays putative osteoblast precursors at the medaka notochordal sheath prior to mineralization, Dev. Biol., 381(1), pp. 134–143.
12. **Q.T. Phan, W.H. Tan, R. Liu, S. Sundaram, A. Buettner, S. Kneitz, et al. (2020),** Cxcl9l and Cxcr3.2 regulate recruitment of osteoclast progenitors to

bone matrix in a medaka osteoporosis model, Proc. Natl. Acad. Sci. U. S. A., 117(32), pp. 19276–19286.

13. **(2009),** Osterix-mCherry transgenic medaka for in vivo imaging of bone formation, Dev. Dyn., (238), pp. 241–248.

14. **J. Renn, C. Winkler (2010),** Characterization of collagen type 10a1 and osteocalcin in early and mature osteoblasts during skeleton formation in medaka, J. Appl. Ichthyol., 26(2), pp. 196–201.

15. **C.V. Pham, T.T. Pham, T.T. Lai, D.C. Trinh, H.V.M. Nguyen, T.T.M. Ha, et al. (2021),** Icariin reduces bone loss in a Rankl-induced transgenic medaka (Oryzias latipes) model for osteoporosis, J. Fish Biol., 98(4), pp. 1039–1048.

SYNERGETIC EFFECTS OF VX-680 AND CURCUMIN COMBINATION ON CANCER CELLS

Bach Thi Hoai Phuong[1], Nguyen Dac Tu[2], Bui Thi Van Khanh[3], To Thanh Thuy[2], Hoang Thi My Nhung[2,3]

ABSTRACT

Objective: *to check if the combination of VX-680 and Curcumin could synergistically induce the anti-tumor effect in three cancer cell lines MCF-7, HeLa, and H1299.* ***Methods:*** *xCelligence system was used to determine the IC50 values, doubling time, and cell behavior.* ***Results:*** *the combination of VX-680 and Curcumin inhibited the proliferation of three cancer cell lines with smaller IC50 values compared to that of the VX-680 and Curcumin alone. Moreover, the mixture led to a significantly higher perturbation rate of the cell cycle than the separate compound.* ***Conclusion:*** *Taken together, VX-680 and Curcumin could be used together to enhance the effect of these compounds on cancer cells.*

Keywords*: Aurora kinases, Aurora kinase inhibitor, VX-680, Curcumin, xCelligence.*

1. INTRODUCTION

In recent years, cancer has become the “hot spot”, which attracts a variety of modern methods and scientists from all over the world, however, it is still an unsolved problem. The Aurora kinase family members (including Aurora A, B, and C) are serine/threonine kinases that match these strict criteria, regulating cell division and multiple signaling pathways [1]. Aberrant Aurora kinase expression might be associated with mitotic errors, resulting in aneuploidy in cells [2]. Over-expression of Aurora kinase is the main cause in some kinds of cancer cell lines (e.g. breast, cervical, non-small cell lung cancer, etc.) according to several publications [3]. Hence, it is not surprising that Aurora kinases have become attractive molecules and their potential in targeted therapy neeeds needs continues to be shed light on. Based on the literature, it is reasonable to classify Aurora kinases as oncogenes. There are 2 main facts: firstly, they are not only aberrantly expressed in one particular type of tumors, like some other oncogenic kinases; secondly, they are involved in a wide variety of cell cycle events, e.g. centrosome function, mitotic entry, kinetochore function, spindle assembly, chromosome segregation, microtubule dynamics, spindle checkpoint function, and cytokinesis [4-7], therefore developing potential Aurora kinase inhibitors as drugs could be promising in the treatment of various cancer.

Based on knowledge about Aurora kinase structure and activity in cells, the compound, VX-680, has been discovered in 2006 in the corporation of Vertex Pharmaceuticals and Merck & Co., being the first Aurora kinase inhibitor to be tested in clinical trials [8-10]. These studies revealed that VX-680 inhibited both Aurora kinase A and B activity, leading to a failure in cytokinesis. This ultimately induces apoptosis – a “safe” death pathway for cancer cells. However, one of the main disadvantages of VX-680 is the long time needed for the induction of polyploidy and apoptosis [8-10]. Curcumin, a natural

[1]National Cancer Hospital
[2]Center of Applied Sciences, Regenerative Medicine, and Advance Technologies, Vinmec Healthcare system,
[3]Faculty of Biology, VNU University of Science, Vietnam National University
*Corresponding to: **Hoang Thi My Nhung**
Email: hoangthimynhung@hus.edu.vn
Received date: 30/8/2022
Reviewed date: 05/9/2022
Accepted date: 15/9/2022

product, is known to have anti-tumor characteristics and can initiate early apoptosis, but it has low targeting ability in the human body [11]. With the hope to increase the efficacy and limit the weakness of each substance, we combined VX-680 and Curcumin (VX-680/Cur) in this project on cancer treatment *in vitro*. This study aimed to (1) evaluate the cytotoxicity, and viability of the new drug combination on different cancer cell lines; and (2) compare the effectiveness of the combination VX-680/Cur to each substance alone.

2. MATERIALS AND METHODS

2.1. Cell lines

In our experiment, we used 3 types of cancer cell lines MCF-7 (breast cancer, HeLa (cervical cancer), and H1299 (lung cancer) as the subjects of research. All of them were obtained from ATCC, cultured in DMEM supplemented with 10% FBS, 1% penicillin/streptomycin in the CO2 incubator at 37^{o}C, 5% CO_2, 95% air.

2.2. Used drugs

VX-680 was purchased from BioVision in colorless liquid form, stock concentration 100 mg/ml in DMSO, stored at -20^{o}C, and protected from light and moisture. The working concentrations of VX-680 used in experiments were 0.8, 0.4, 0.2, 0.1, and 0.05 (µM), diluted in 0.1% DMSO.

Curcumin was obtained from Merck in form of an orange-yellow powder. It is soluble in DMSO and stored between 15^{o}C and 30^{o}C. The working concentrations of Curcumin used in experiments were 80, 40, 20, 10, and 5 (µM), diluted in 0.1% DMSO.

The combination of VX-680 and Curcumin (VX-680/Cur) with the ratio: 0.8/80; 0.4/40; 0.2/20; 0.1/10; 0.05/5 (µM), respectively. These compounds are dissolved in 0.1% DMSO, having yellow color due to the natural color of Curcumin.

2.3. Real-time monitoring of cell proliferation using xCELLigence technology

A real-time cell analyzer (RTCA) is a technique that uses real-time cell monitoring to detect migration, cytotoxicity, adherence, and proliferation of cells during direct and indirect co-cultures. This xCELLigence system was developed by the partnership between Roche Applied Science (Quebec, Canada) and ACEA Biosiences Inc. (San Diego, CA, USA). Its principle is to monitor cell events in real-time by measuring electrical impedance across gold-plated sensor electrodes that are placed at the bottom of the E-Plate 96.

There were 4 main steps in using this system.

Step 1: Checking the signal of E-Plate 96 without the presence of cells for 1 minute to make sure that the Cell Index (CI) of all wells of the plate is set to zero point, set value as background.

Step 2: Each cell type was seeded at a density of 4,000 cells in 200 µL medium/well. These cells started to adhere and proliferate normally for 24 hours.

Step 3: Before the addition of compounds, the Cell Index curves were normalized to a time point in order to possess the same status before being exposed to the compounds. Then, VX-680, Cur, and VX-680/Cur were added to E-Plate 96 with a range of different concentrations.

Step 4: After CI of control went totally to 0, we switched off xCELLigence RTCA SP instrument; we obtained RTCA software from Roche to analyze data. Quantification via the RTCA software allows the plotting of a sigmoidal dose-response curve and automatically calculates a half inhibitory concentration (IC50) after 120 hours of the experiment.

2.4. Cytell Cell Imaging System

The Cytell Cell Imaging System combines the functionalities of a digital microscope, an image cytometer, and a cell counter in a single benchtop instrument. This compact, application-driven, automated cell imaging system provides

robust quantitative results using preconfigured biological applications (BioApps). Each BioApp is an easy-to-use, automated module that covers all steps of a specific biological application or assay. Cytell Cell Imaging System comes bundled with 5 BioApps to simplify routine cell lab tasks while providing high-quality scientific data. We used the Automated Imaging BioApp to visualize the nuclear area of cells. It can reveal the morphology and density of cells.

- Step 1: Incubation cells in a 96-plate with Reagent G which can enter and stain the nucleus.
- Step 2: Setting up protocol with suitable wavelength, focus and exposure settings.
- Step 3: Clicking Edit to check that settings are optimal for the current sample
- Step 4: Run to immediately start the automatic collection of a series of images.

3. RESULTS AND DISCUSSIONS

3.1. The effect of VX-680/Cur on the proliferation of three cancer cell lines

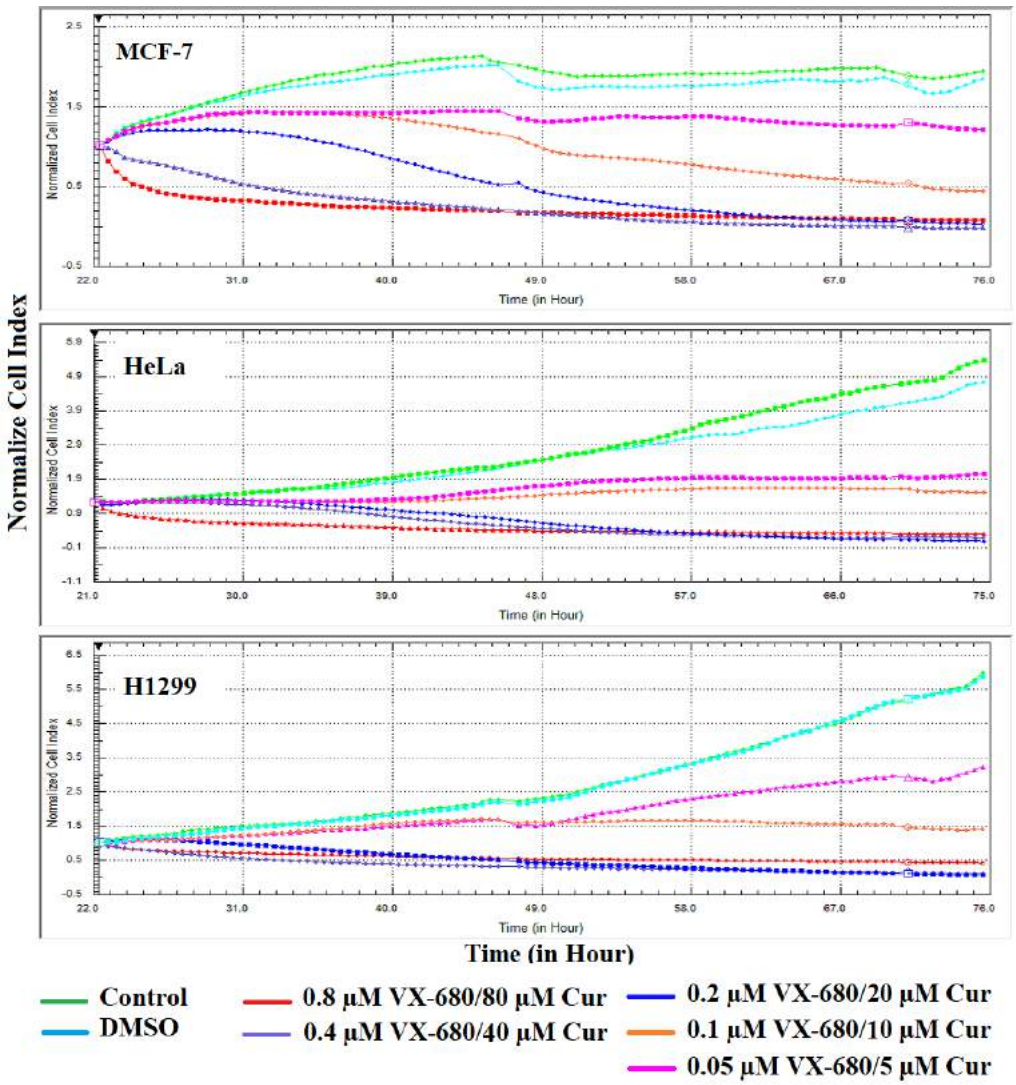

Figure 1. Real-time cellular analysis profiling of MCF-7, HeLa, and H1299 cells treated with 5 concentrations of VX-680/Cur

A glance at Figure 1 reveals that there are several important characteristics of the growth curves, which are similar for all cancer cell lines. In detail, firstly, control cells or cells with 0.1% DMSO have the fastest increase in the Normalize Cell Index (NCI) for 54 hours. The normal growth curves in presence of DMSO confirmed the fact that cells are not influenced by solvent.

Secondly, after an approximately 10-hour treatment, at the highest and lowest concentration of VX/Cur (0.8uM/80uM and 0.05uM/5uM), cell curves have whether an immediately downward trend even reached zero, or a parallel upward trend with biological control, respectively. It reveals that while 0.8uM/80uM exerted the strongest cytotoxicity leading to totally cell population death, 0.05uM VX-680/5uM Cur had weak cytotoxicity resulting in the continued growth of the cell population so they did not exhibit a desirable effect on cells. Furthermore, cells treated with this combination obeyed dose–response regulation: the higher concentration, the more toxic drugs made cell change.

Thirdly, regarding the concentration of 0.2uM VX-680/20uM Cur, NCI seemly experienced a drop to 0 gradually after remaining unchanged from 22h to 31h. When NCI is stabled during this period, it means that cells did not grow or die. This event was probably caused by cell cycle arrest at interphase. On the other hand, the concentration might not affect too strong or weakness of the cancer cell, interestingly it induced cell death progressively so it was chosen for the appropriate concentration in the next analyzing step.

3.2. The different characteristics in cell response between 3 cell lines

Although the different cell lines have many common features, there still exist many significant differences after careful analyses. First and foremost, we can easily realize a dramatic fall of 0.4uM VX-680/40uM Cur in Figure 1 but the time point when this growth curve met the curve of the highest concentration was at 47h, 52h for MCF-7 and HeLa cells, respectively, while no significant difference was observed for H1299 cells. It means that MCF-7 cells had the shortest time, after that were HeLa and H1299 cells in order to gain cytotoxicity equal to the strongest concentration (0.8uM VX-680/80uM Cur). Moreover, in MCF-7 cells while the NCI of 0.1uM VX-680/1uM Cur witnessed a considerable decline to nearly 0.5 after hitting a peak at approximately 1.5, the same treatment on HeLa and H1299 cell lines resulted in a more stable curve, fluctuating around 1.5 during almost the whole time. From these results, we can put forward the prediction that there might have a factor that is different from each cancer cell line, governed cell response to this drug, and p53 – a “guardian of the genome” could be the target. The reason lies in MCF-7 cell line has a normal expression of p53 [12], whilst HeLa and H1299 cell lines have weaker [13] or no expression of it [14], respectively. Hence, when Curcumin and VX-680 activate the p53 pathway, the effect is predominantly expressed in cells that have p53 expression.

3.3. Comparison of the effectiveness of the combination VX-680/Cur and each separate substance

One of the distinct trends today in cancer treatment is combination chemotherapy, which means that drugs with different effects are combined, not only increasing activity but also overcoming resistance [15]. An attractive example of efficacy is a combination of nutlin-3 and VX-680 selectively targets p53 mutant cells while protecting the human normal cell line [9]. Nevertheless, in some cases, the combination did not show good results, for instance, Actinomycin D can protect both normal fibroblasts and p53 mutation cancer cell lines from VX-680-induced polyploidy [10]. Therefore, we must check our combination VX-680/Cur can bring real effect to each cell line and be compared to each component.

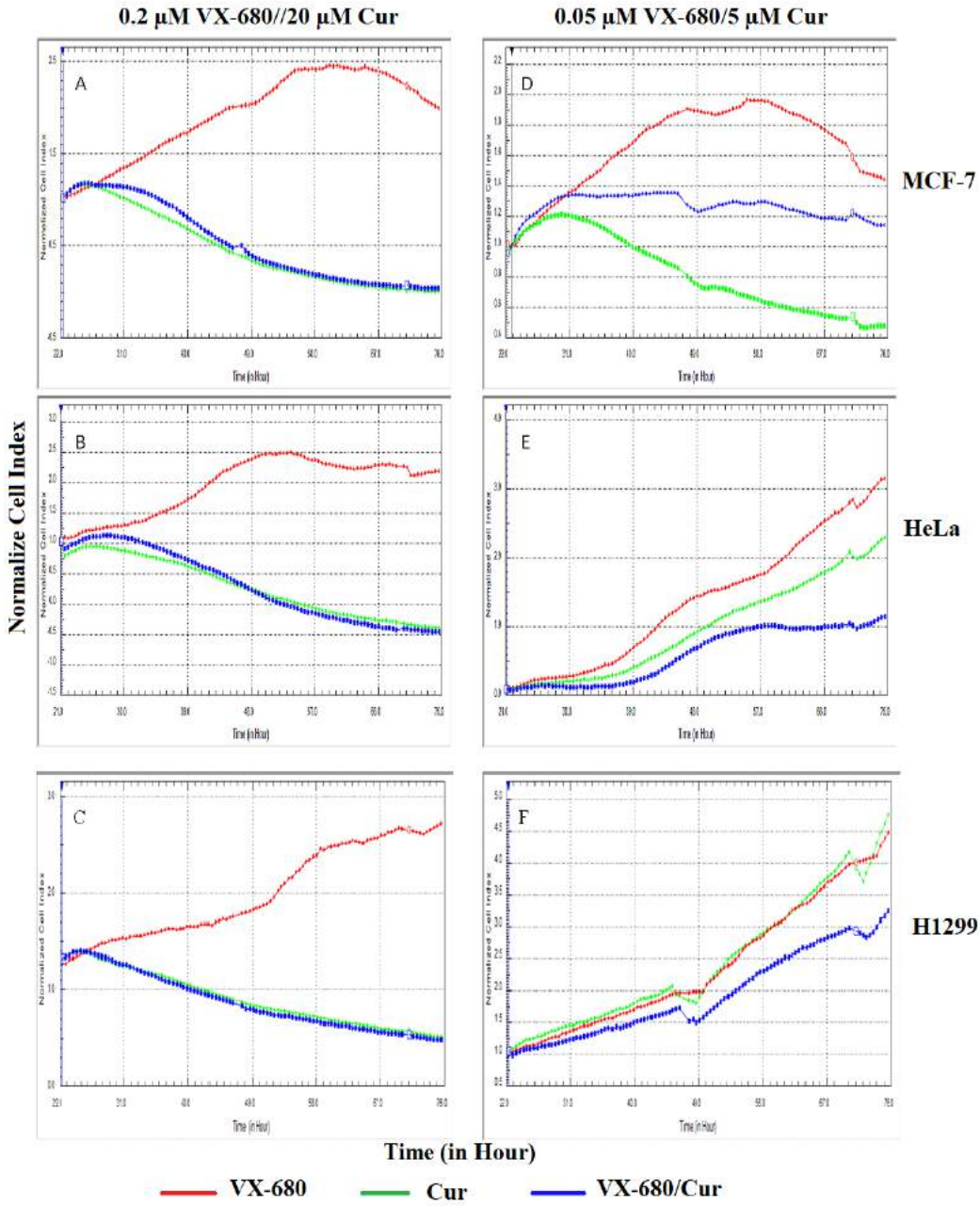

Figure 2. Real-time cellular analysis profiling of MCF-7, HeLa, and H1299 cells treated with 2 concentrations of VX-680, Cur and-680/Cur (0.2uM/20uM: left; 0.05uM/5uM: right) for 76h experiment hours.

As clearly seen in Figure 2, at the concentration of 0.2uM VX-680/20uM Cur and 20uM Cur alone, a similar cell response curve was shown, which decreased fast after a short delay time. Surprisingly, for both MCF-7 and HeLa cells, NCI of combination samples declined slower than NCI of Cur from 25h to 48h, nevertheless, they met each other after 24h, suggesting that at high concentration Curcumin has a stronger effect than VX-680 in combination to these cancer cells. As the similar pattern

of this drug system and Cur effect at high concentration, we continuously evaluated at a lower concentration, 0.05uM VX-680/5uM Cur and Curcumin with the same concentration in the combination. In MCF-7 cell line, the concentration of VX-680/Cur led to an immediate fall of the NCI under 1.2 points after remaining stable at nearly 1.6 within 16 hours. By contrast, Cur's curve decreased more rapidly after peaking at 1.2 at 31h in comparison with the combination. Furthermore, the corresponding amount of Cur made NCI rose sharply and hit a peak at 3.2 and 4.75 in HeLa and H1299 cell lines, leaving VX-680/Cur climbing gradually with maximum NCI being only 2.0 and 3.3 approximately, respectively. It reveals that might VX-680 effect is expressed more clearly in HeLa and H1299 cell lines at low concentrations when combined with Curcumin. The 2 opposite pictures of VX-680/Cur in MCF-7 and 2 other types of cell can be explained by the fact that VX-680 preferentially has a better effect in p53- compromised cancer cell lines [9], therefore its effect combined with Cur exerted stronger efficacy as compared with pure Cur in HeLa and H1299 cell. Importantly, whether high or low concentration VX-680/Cur still demonstrated higher effects regarding cell growth inhibition compared to VX-680.

3.4. Doubling time

During the time from 22h to 76h, the data demonstrates the effect on the doubling time of the 3 substances on each cell line. Firstly, it cannot be denied that the doubling time of MCF-7 cells is totally different compared to the other cell lines. For example, the value is negative after adding Cur and VX/Cur while a positive value is observed after adding pure VX-680, suggesting that the former may inhibit cell proliferation more effectively than the latter.

For HeLa cell line, the doubling time positive value of VX-680/Cur is higher than both pure VX-680 and Curcumin treatment alone. It proved a fact that cells took a longer time to grow: 40 hours than about 25 hours or nearly 30 hours to duplicate in the sample adding with VX-680/Cur, VX-680, and Cur, respectively. Similarly, we can easily see the upward trend of positive doubling time from VX-680, Cur to VX-680/Cur in H1299 cell line. It might be explained that VX-680 inhibits Aurora kinase expression – a key factor that controls cell division. As a result, the time needed for cell doubling is longer than each substance alone (Figure 3).

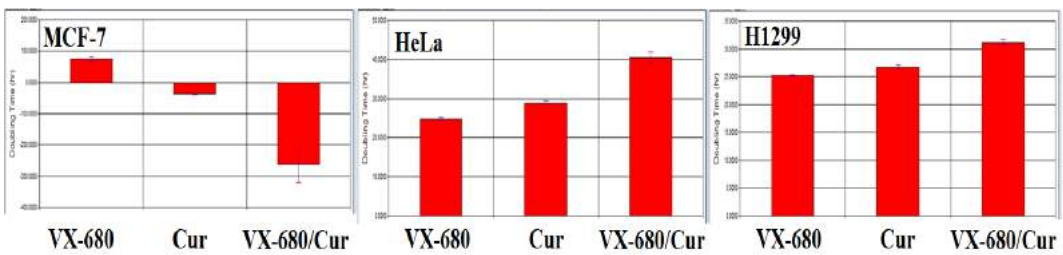

Figure 3. Doubling time of cells treated with the 3 substances from 22h to 76h

3.5. Cytotoxicity of drugs on cancer cell lines

We evaluate the cytotoxicity of these drugs by determination of IC50 values. According to the FDA, IC50 represents the concentration of drug that is required for 50% inhibition in vitro. The lower the IC50 value, the more toxic is the drug. Taking advantage of the xCELLigence system, we determined the IC50 value of each substance on each cell line as summarized in Table 1.

Table 1. IC50 values of 3 substances on three cancer cell lines after 146h exposure

Cell Type / Substance	MCF-7	HeLa	H1299
VX-680	0.379 µM (R^2=90.65%)	0.184 µM (R^2=96.03%)	0.132 µM (R^2 =99.89%)
Cur	7.194 µM (R^2=99.66%)	9.021 µM (R^2=99.64%)	9.575 µM (R^2=99.98%)
VX-680/Cur	0.099 µM (R^2=99.99%)	0.056 µM (R^2=98.87%)	0.086 µM (R^2 =99.98%)

As shown clearly in the table, IC50 of VX-680/Cur is smaller than VX-680 or Cur alone, suggesting that the combination treatment expressed more effectiveness for inhibition of cancer cell proliferation as compared to each substance alone. Interestingly, the difference between IC50 of VX-680/Cur and VX-680 is 0.28uM in MCF-7, being much higher than for HeLa (0.128uM) and H1299 (0.046uM) cells. These numbers confirm the better effectiveness of the combination treatment on MCF-7 cells compared to HeLa and H1299 cells.

3.6. Perturbation of cell cycle in the presence of three compounds

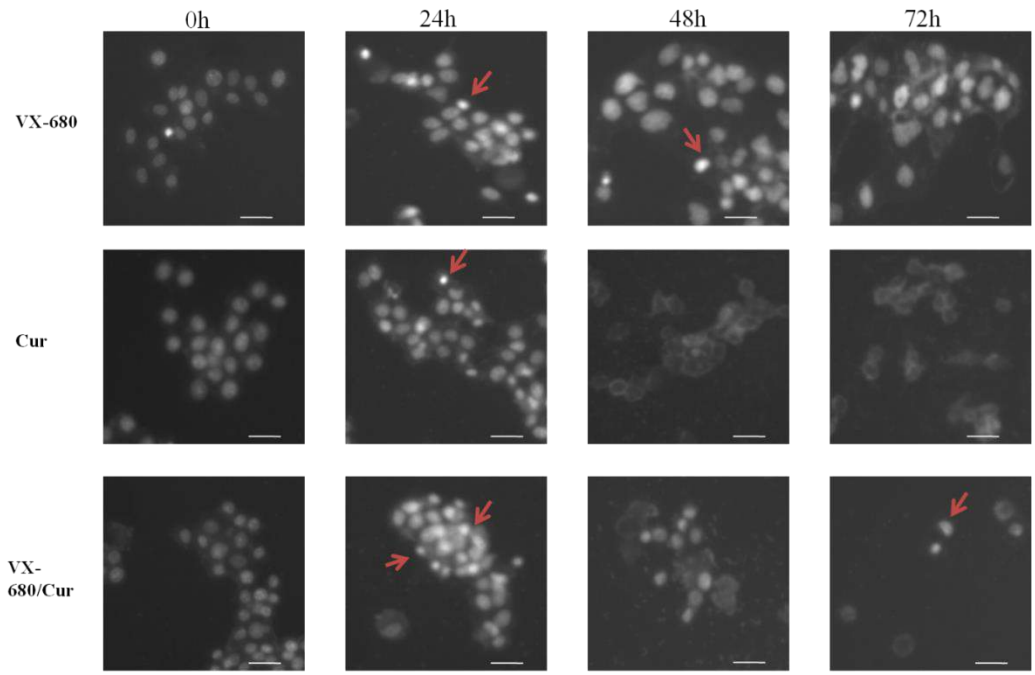

Figure 4. Automated image acquisition after treatment MCF-7 cells with each substance at 4-time points: 0h, 24h, 48h, and 72h at 0.2uM VX-680/20uM Cur. (Bar scale: 20µm)

As discussed in the xCELLigence results, we supposed that cells treated with VX-680/Cur were arrested at the interface and cell death is subsequently triggered during the following hours. We incubated the cells with reagent G, a fluorescent dye, which can enter the nucleus and bind to DNA. This not only marks the location of the

nucleus but also reveals its morphology and the intensity of the staining correlates with the DNA content allowing to determination of cell cycle phases. Based on our prediction of different p53 expressions in the first experimental analysis, we would like to examine the cell images on two cell lines: MCF-7 cells with normal expression of p53 and H1299 cells with a total absence of p53 expression at 0.2uM VX-680/20 uM Cur. As the first step, we observe the morphology and cell density of the control sample with or without 0.1% DMSO, as illustrated in Figure 16. MCF-7 cells have a small size and gather in a group, whilst H1299 cells have a bigger size and are distributed equally on a disk surface.

Regarding the cells treated with VX-680 for both cell lines, experimental results clearly show that the nucleus area was significantly enlarged at 48h, especially for the H1299 cell line. The nucleus became multi-lobed, often with a high DNA content. These phenomena could be due to a process termed “mitotic slippage” which can be induced by anti-mitotic drugs that inhibit microtubule organization and serine/threonine kinases. In detail, through inhibiting Aurora kinases, VX-680 may activate the spindle assembly checkpoint (SAC) and cause cell arrest at M phase. However, some cells may escape from checkpoint arrest and enter G1 phase without having completed chromosome segregation and cytokinesis. Slipped cells have replicated their DNA in S phase, forming hyperploid cells; the process is called endoreduplication [17]. Nuclear envelopes, in turn, are formed around random groups of chromosomes as they decondense, consequently producing what was known as “restitution nuclei”; and cells became multinucleated [5]. The higher rate of the big nucleus means polyploidy occurs frequently; the more cells will escape from the cell cycle checkpoint. Hence, this rate needs to be decreased in parallel with apoptosis increase.

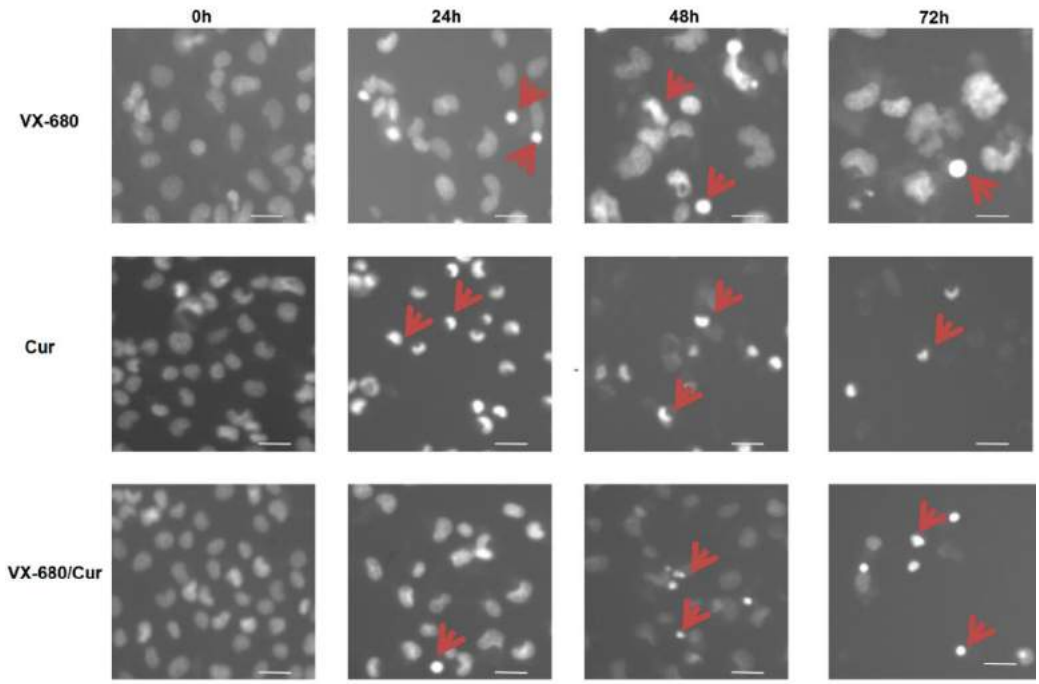

Figure 5. Automated images acquisition after treatment H1299 cells with each substance, at 4-time points: 0h, 24h, 48h, and 72h at 0.2uM VX-680/20uM Cur. (Bar scale: 20μm).

By contrast, we can easily recognize smaller condensed nuclei of cells after treatment with Curcumin. Besides the tiny nucleus size, there was a lot of cell debris. At 48h and 72h time points, there was no more nucleus staining for MCF-7 cells, and only some condensed nuclei were observed in the other cell lines, suggesting that Curcumin might activate cell death quickly, especially in the MCF-7 cell line possibly by several mechanisms such as p53 - dependent and p53 – independent pathway when exposed with Curcumin.

Interestingly, cells exposed to VX-680/Cur have small size nuclei like after Cur treatment and the staining intensity decreases over time. On the other hand, the density of cells at 72h for MCF-7 cell line is lower than for the H1299 cell line, in detail: there were faintly stained nuclei with debris in MCF-7 cells instead of condensed nuclei in H1299 cell line. These facts could be explained by 3 reasons: (1) Curcumin promoted VX-680 activities through suppression of Aurora kinases, so VX-680/Cur induced higher cytotoxicity and produced a more complete influence on enzyme activities than VX-680 did alone. However, the concentration of Cur is just 2x the IC50 of Cur so in this concentration combination, the effect of Cur may be more pronounced than VX-680. (2) Curcumin was proved to be able to arrest cells at G1/S, so VX-680/Cur probably decreased the number of cells undergoing M phase, hence, the number of cells treated with this combination is becoming smaller than after treatment with VX-680 alone; (3) MCF-7 cells have normal p53 expression while H1299 cells do not express p53 due to a partial deletion of the p53 gene, so when Curcumin activates the p53 pathway, the MCF-7 cell line will react better than the H1299 cell line.

4. CONCLUSION

In conclusion, VX-680/Cur exerted stronger effects due to the synergism between VX-680 and Curcumin. This result agreed with the xCELLigence analysis.

Acknowledgment

We thank staffs of CELIFE, Faculty of Biology, VNU University of Science for assistance in microscopic imaging and Center of Applied Sciences, Regenerative Medicine, and Advance Technologies, Vinmec Healthcare system,

REFERENCES

1. **Bolanos-Garcia, V.M. (2005)**. Aurora kinases, Int J Biochem Cell Biol, 37 (8), pp. 1572-1577.
2. **Giet, R., Mclean D., et al. (2002)**. Drosophila Aurora A kinase is required to localize D-TACC to centrosomes and to regulate astral microtubules. J Cell Biol, 156 (3), pp. 437-451.
3. **Dar, A.A., Zaika A., et al. (2008).** Frequent overexpression of Aurora Kinase A in upper gastrointestinal adenocarcinomas correlates with potent antiapoptotic functions. Cancer, 112 (8), pp. 1688-1698.
4. **Andrews, P.D., Ovechkina Y., et al. (2004).** Aurora B regulates MCAK at the mitotic centromere. Dev Cell, 6 (2), pp. 253-268
5. **Blagosklonny, M.V. (2007).** Mitotic arrest and cell fate: why and how mitotic inhibition of transcription drives mutually exclusive events. Cell Cycle, 6 (1), pp. 70-74
6. **Carmena, M., Ruchaud S., and Earnshaw W.C. (2009).** Making the Auroras glow: regulation of Aurora A and B kinase function by interacting proteins. Curr Opin Cell Biol, 21 (6), pp. 796-805
7. **Cazales M., S.E., Montembault E., Dozier C., Prigent C., Ducommun B. (2005).** CDC25B phosphorylation by Aurora-A occurs at the G2/M transition and is inhibited by DNA damage. Cell Cycle, 4, pp. 1233-1238
8. **Harrington, E.A., Bebbington D., et al. (2004).** VX-680, a potent and selective small-molecule inhibitor of the

Aurora kinases, suppresses tumor growth in vivo. Nat Med, 10 (3), pp. 262-267.

9. **Cheok, C.F., Kua N., Kaldis P., and Lane D.P. (2010).** Combination of nutlin-3 and VX-680 selectively targets p53 mutant cells with reversible effects on cells expressing wild-type p53. Cell Death Differ, 17 (9), pp. 1486-1500
10. **Rao, B., Van Leeuwen I.M., et al. (2010).** Evaluation of an Actinomycin D/VX-680 aurora kinase inhibitor combination in p53-based cyclotherapy. Oncotarget, 1 (7), pp. 639-650
11. **Gupta, S.C., Prasad S., et al. (2011).** Multitargeting by curcumin as revealed by molecular interaction studies. Nat Prod Rep, 28 (12), pp. 1937-1955.
12. **Wasielewski, M., Elstrodt F., Klijn J.G., Berns E.M., and Schutte M. (2006).** Thirteen new p53 gene mutants identified among 41 human breast cancer cell lines. Breast Cancer Res Treat, 99 (1), pp. 97-101
13. **Scheffner, M., Munger K., Byrne J.C., and Howley P.M. (1991).** The state of the p53 and retinoblastoma genes in human cervical carcinoma cell lines. Proc Natl Acad Sci U S A, 88 (13), pp. 5523-5527
14. **Lai, S.L., Perng R.P., and Hwang J. (2000).** p53 gene status modulates the chemosensitivity of non-small cell lung cancer cells. J Biomed Sci, 7 (1), pp. 64-70

In vitro Angiogenesis Capacity of Mesenchymal Stem Cells Derived from Umbilical Cord Blood and Adipose Tissue

Do Thi Xuan Phuong[1,2], Than Thi Trang Uyen[2], Dinh Duy Thanh[1,3], Hoang Thi My Nhung[1], Do Xuan Hai[4]

ABSTRACT

Objective: *Angiogenesis plays an essential role in regenerative medicine and damaged tissue repair. Mesenchymal stem cells (MSCs) have been demonstrated to have angiogenic properties and therapeutic potential through their capacity to induce endothelial cell proliferation and tube formation. Besides, bone marrow-derived MSCs have been reported to form a tube-like structure on the Matrigel. In this study, we aimed to check the ability of adipose (AD) and umbilical cord blood (UCB) – derived MSCs in the tube formation and compare them to that of human umbilical cord vein endothelial cells (hUVECs).* ***Methods:*** *The Matrigel was used for the in vitro angiogenesis model.* ***Results:*** *We successfully isolated and cultured ADMSCs, UCBMSCs, and hUVECs with the high expression of specific cell type markers. Moreover, hUVECs could form a tube-like structure network and maintain this morphology for more than 8 hours. ADMSCs and UCBMSCs were able to form the tube-like structure at the early time of 2 hours but failed to retain the structure.* ***Conclusion:*** *ADMSCs and UCBMSCs had potential in the formation of tube-like structures in a short time.*

Keywords: *hUVECs, ADMSCs, UCBMSCs, angiogenesis, Matrigel.*

1. INTRODUCTION

The formation of new blood vessels from existing vasculature is crucial for many physiological activities, such as wound healing, growth, and functioning of the female reproductive organs [1]. Disordered angiogenic mechanisms, including excessive and impaired angiogenesis, are involved in several diseases: cancer, psoriasis, arthritis, retinopathy, obesity, asthma, atherosclerosis, *etc.* [2]. Therefore, angiogenesis research could lead to potential cures or treatments for such diseases.

Mesenchymal stem cells (MSCs) have been reported to have proangiogenic features [3]. These cells can enhance *de novo* vessels formation by endothelial colony-forming cells [4] and stabilize the endothelial network [5]. In murine, bone marrow-MSCs have been shown to significantly impact hematopoietic stem cell proliferation, survival, and homing [6]. Recently, bone marrow-derived MSCs demonstrated the *in vitro* angiogenesis capacity on Matrigel [7]. That implies the similar angiogenic property of other MSC types; however, this has not been well elucidated. In this study, we aimed to evaluate the *in vitro* angiogenesis capacity on Matrigel of adipose-derived MSCs (ADMSCs) and umbilical cord blood-derived MSCs (UCBMSCs).

[1]Faculty of Biology, VNU University of Science
[2]Regenerative Medicine, and Advance Technologies, Vinmec Healthcare system
[3]Laboratory for Organogenesis and Regeneration, GIGA-R, University of Liège
[4]Department of Practical and Experimental Surgery, Vietnam Military Medical University
Corresponding to: **Do Xuan Hai**
Email: doxuanhai.vmmu@gmail.com
Received date: 30/8/2022
Reviewed date: 10/9/2022
Accepted date: 15/9/2022

2. MATERIALS AND METHODS

2.1. Mesenchymal stem cell isolation and culture

Cord blood units were collected at Vinmec International General Hospital with donor consents. All samples will be tested to ensure they are free of HIV, HBV, HCV, and HPV. Blood units were also disinfected immediately after collection and before handling. Blood mononuclear cells were isolated by density centrifugation using Ficoll-Paque 430 × g/30 min/ 20°C, then seeded into culture dishes with StemMACS™ MSC medium (Miltenyi Biotec, Bergisch Gladbach, Germany). At the same time, plasma from the blood sample was collected, then used to coat the culture plate's surface and add to the culture medium.

Adipose tissue samples were collected by plastic surgeons at Vinmec International Hospital using the suction method with donor consents. Samples are sterilized before entering the laboratory. Adipose tissue was washed 2-3 times with PBS by centrifugation at 500 × g/ 10 min/ 20°C to remove red blood cells and collect the

supernatant fat layer. Tissues were incubated with 200 U/mL collagenase type I (Gibco, Massachusetts, USA) diluted in HBSS and 0.1% human albumin for 1h at 37°C. Cells were collected by centrifugation at 500 × g/10 min/ 20°C, the supernatant was removed, and cell residues were dissolved in StemMACS™ MSC culture medium (Miltenyi Biotec, Bergisch Gladbach, Germany). Cells were seeded at a density of 5000 cells/cm^2 into a T75 culture flask coated with CTS™ CELLstartTM (Gibco, Massachusetts, USA) (diluted in PBS at 1:100 ratio), culture at 37°C and 5% CO2.

2.2. Human umbilical vein endothelial cells isolation and culture

The umbilical cords were collected in the operating room of Vinmec Times City International Hospital with the consent of the family. The umbilical cords were washed with 70% ethanol and then PBS to disinfect and remove blood. A needle was used to inject PBS through the umbilical vein to wash and remove the venous blood. The vein was then injected with 500 U/mL collagenase type I (Gibco, Massachusetts, USA) diluted in HBSS and 0.1% human albumin and incubated at 37°C for 15 minutes. The intravenous solution was then collected and centrifugated at 1200 rpm/10 min. Cell residues were mixed with EGM-2 culture medium (Lonza, Basel, Switzerland) and seeded at a density of 5000 cells/cm^2 in a T75 culture flask coated with CTS™ CELLstart™ (Gibco, Massachusetts, USA) diluted in PBS 1:100 ratio. After two days, the medium was replaced, and the floating cells were removed.

2.3. Immunophenotyping analysis

When MSCs reached 80% confluence at the second subculture, cells were harvested using CTS™ TrypLETM (Thermo Fisher Scientific, USA). Cells were used for biomarker analysis using the Human MSC Analysis kit (BD Biosciences, California, US). The kit included: MSC positive cocktail (CD90 FITC, CD105 PerCP-CyTM5.5, and CD73 APC), and negative MSC cocktail (PE: CD45, CD34, CD11b, CD19 and HLA-DR) according to the manufacturer's instructions. Flow cytometry analysis was performed on a Beckman Coulter flow cytometer and analyzed with the Navious software.

hUVECs at passage 2 were also harvested using CTS™ TrypLE™ (Thermo Fisher Scientific, USA). Cells were stained with antibodies against the positive surface marker CD31-FITC, CD146-FITC, CD105-PerCP Cy5.5 (Miltenyi Biotec, Bergisch Gladbach, Germany) and negative surface marker CD90-FITC (BD Biosciences, California, US), Myosin heavy chain-APC (Miltenyi Biotec, Bergisch Gladbach, Germany) according to the manufacturer's instructions. Flow cytometry analysis was performed on a Beckman Coulter flow cytometer and analyzed with Navious software.

2.4. Multi-lineage differentiation

Osteogenesis differentiation

MSCs were cultured for at least two weeks in an osteogenic differentiation medium (STEMPRO Osteogenesis Differentiation Kit, Thermo Fisher Scientific, USA), then washed with PBS and fixed with 4% paraformaldehyde for 30 min at room temperature. Cells were rewashed with distilled water and stained with 2% Alizarin Red S (pH=4.2) for 2-3 min at room temperature, then rinsed with distilled water. Cell examination and photographing were done on an inverted microscope (Olympus, Japan).

Chondrogenesis differentiation

5 µl of MSCs cell suspension (10^7 cells/ml) was dropped into each well of 96 well plate and incubated at 37°C, 2% CO2 for cell adhesion, then gently added cartilage differentiation medium (STEMPRO Chondrogenesis Differentiation Kit, Thermo Fisher Scientific, USA) and cultured for at least two weeks. The cells were then washed with PBS and fixed with 4% paraformaldehyde for 30 min at room temperature. Cells were rewashed with PBS and stained with 1% Alcian Blue solution in 3% acetic acid (pH = 2.5) for 30 min at room temperature, then rinsed again with 0.1 N HCl and distilled water. The cells were examined and photographed on an inverted microscope (Olympus, Japan).

Adipogenesis differentiation

MSCs were cultured for at least two weeks in adipogenic differentiation medium (STEMPRO Adipogenesis Differentiation Kit, Thermo Fisher Scientific, USA), then washed with PBS and stained with Oil Red O solution (diluted proportionally with distilled water 1 Oil Red O: 2 distilled water) for 15 minutes at room temperature. Before staining, cells were fixed with 4% paraformaldehyde for 30 min at room temperature. Cell imaging was done on an inverted microscope (Olympus, Japan).

2.5. Angiogenesis assay

In vitro angiogenesis of MSCs and hUVECs on Matrigel were evaluated using the Angiogenesis Assay Kit (In Vitro) (Abcam, UK) according to the supplier's instructions. In negative control wells, hUVEC cells in EGM-2 were supplemented with 10 µM Suramin (angiogenesis inhibitor). The background was the cell-seeded

into the CTS™ CELLstart™ coat well (Gibco, Massachusetts, USA) (diluted in PBS 1:300). Angiogenesis was monitored for 10h according to the supplier's instructions and photographed under a fluorescence microscope (Olympus, Japan). Image and quantification were done using Image J 1.53q.

2.6. Statistical analysis

Statistical significance between groups was assessed using Anova with a p-value threshold of 0.05.

3. RESULTS and DISCUSSIONS

3.1. Characterization ADMSCs and UCBMSCs

After isolation, both cell types were cultured in the completed StemMACS culture medium. For UCBMSCs, the medium was supplemented with 10% of autologous plasma. The fibroblast-like cells appeared after 24 hours of cultivation in ADMSCs culture (Figure 1A). In UCBMSCs, after two weeks, there were few clusters of adherent cells detected (Figure 1B). The morphology of both cell types was similar when the cells reached the higher confluence, with the fibroblast-like shape (Figure 1B, C). Because the percentage of MSCs in cord blood was marginal (below 1%) [8] compared to that in adipose tissue (1×10^6cells/1gram adipose tissue) [9], the detecting and isolating of MSCs from these two sources were accordingly different. Our study was consistent with the previous paper of Liem et al. [10], which indicated that it takes about 5-25 days to successfully isolate MSCs from human umbilical cord blood.

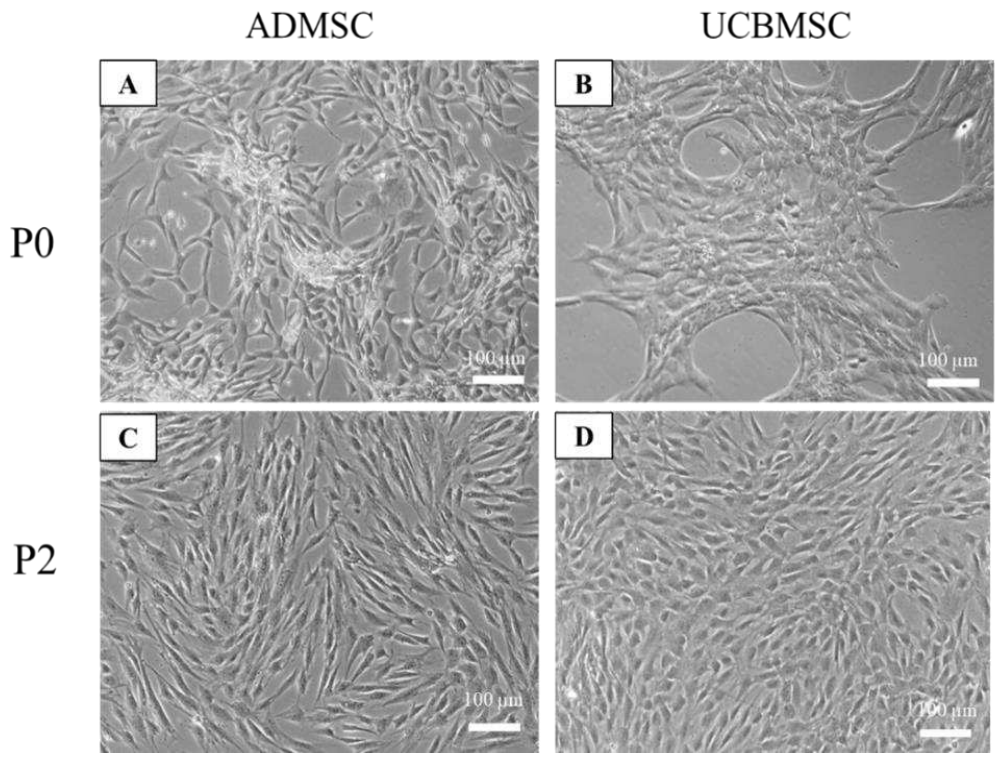

Figure 1. The morphology of ADMSCs and UCBMSCs at different passages. (A) ADMSCs at passage 0 (P0). (B) UCBMSCs at P0. (C) ADMSCs at P2. (D) UCBMSCs at P2.

When the cells reached the adequate number at P2, with 80% of confluence, they were collected for the immunophenotyping analysis and the differentiation capacity evaluation. As shown in Figure 2, both cell types expressed a high percentage of MSC-positive markers and a very low percentage of MSC-negative markers. The expression of CD105, CD90, and CD73 in ADMSCs was more than 99% (Table 1). Similarly, UCBMSCs expressed more than 99% of CD105 and CD90 but were slightly lower for CD73 with 96.2% (Table 1). Besides, the expression of negative markers was 0.125 % in ADMSCs, and 1% in UCBMSCs (Table 1). These MSCs satisfied the standard requirements for MSCs proposed by the International Society for Cellular Therapy (ISCT) (2006), with adhesion ability, high expression of MSC positive markers (> 97%), and lack of negative markers (< 1%) [11].

Table 1. The immunophenotype of ADMSCs and UCBMSCs (n=3)

Cell type		**ADMSCs**	**UCMSCs**
Positive markers (%)	CD73	99.9 ± 0.071	96.2 ± 1.697
	CD90	99.9 ± 0.028	99.95 ± 0.071
	CD105	99.02 ± 0.028	99.95 ± 0.071
Negative marker cocktail (%)		0.125 ± 0.035	1 ± 1.131

In the meantime, we evaluated the multi-lineage differentiation of ADMSCs (Figure 2C) and UCBMSCs (Figure 2D). Both cell types showed the ability to differentiate into osteoblasts, chondrocytes, and adipocytes. The cells were positive with Alizarin Red staining indicating the calcium deposition in the osteoblasts. These cells also carried the lipid droplets in the cytoplasm, which were positive with Oil Red O staining in the adipogenesis medium. Moreover, in the chondrocyte differentiation condition, the cells gathered into the cartilage-like structure and were positive with Alizarin Blue staining. These results mean that ADMSCs and UCBMSCs in this study had tri-lineage capacity into bone, cartilage, and fat. This character was also the standard criteria for the mesenchymal stem cell definition of ISCT [11]. Taken together, our results demonstrated that we successfully isolated and cultured mesenchymal stem cells from adipose tissue and umbilical cord blood.

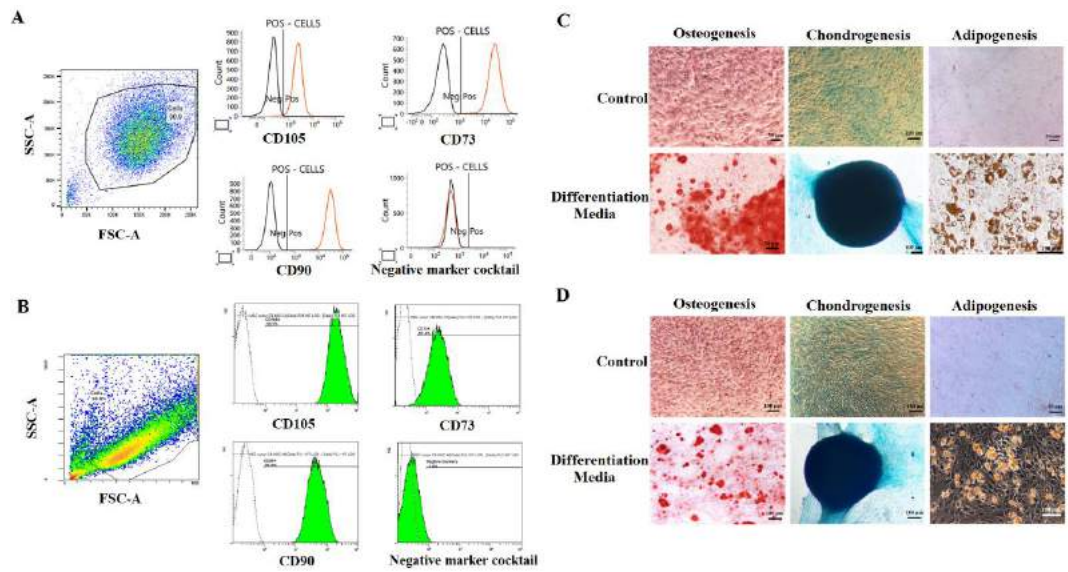

Figure 2. The immunophenotype and the differentiation capacity of ADMSCs and UCBMSCs. (A) The expression of positive and negative markers in ADMSCs. (B) The expression of positive and negative markers in UCBMSCs. (C) The differentiation of ADMSCs to osteoblasts, adipocytes, and chondrocytes. (D) The differentiation of ADMSCs to osteoblasts, adipocytes, and chondrocytes.

3.2. Isolation and characterization of hUVECs

We used the enzyme digestion method for the isolation of hUVECs. The collected cells were grown in the EGM-2 culture medium on a CellSart-coating plate. After two days of seeding, cells started adhering to the culture surface with a polygonal cell shape (Figure 3A). Cells in P2 were collected for the immunophenotype analysis. The data showed that these cells expressed CD31 (99.23 ± 0.42 %), CD146 (99,7 ± 0,1%), and CD105 (99,5 ± 0,53%). These markers are reported as endothelial markers in previous studies [12]. Moreover, our isolated cells were negative for CD90 marker (0,6 ± 0,32%), and myosin heavy chain (0,74 ± 0,4%) (Figure 3B, C). These data indicate that we successfully isolated endothelial cells from human umbilical cord veins.

Table 2. The expression of endothelial cell markers at passage 2 (n=3).

Positive markers (%)	CD31	99.23 ± 0.42
	CD146	99.7 ± 0.1
	CD105	99.5 ± 0.53
Negative markers (%)	CD90	0.6 ± 0.32
	Mouse heavy chain	0.74 ± 0.4

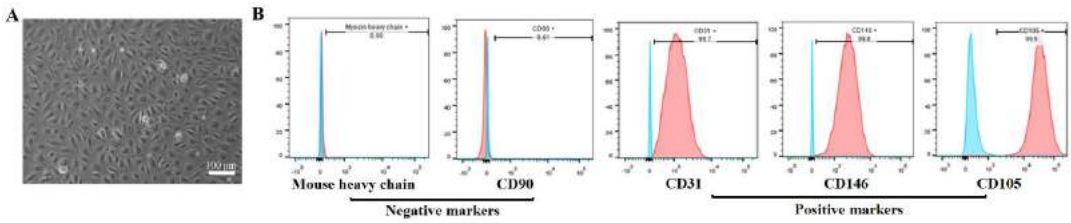

Figure 3. Characterization of hUVECs. (A) The morphology of isolated cells at passage 0. (B) The immunophenotype of isolated cells at passage 2.

3.3. *In vitro* angiogenesis of ADMSCs and UCBMSCs on Matrigel

Angiogenesis assays are important tools for both mechanistic study and therapeutic development. *In vivo* angiogenesis tests are considered the most informative but expensive and time-consuming, requiring intensively trained personnel. On the other hand, *in vitro* tests tend to be faster, less expensive, and easier to interpret. *In vitro* angiogenesis assays operate on the principle that endothelial cells form a tube-like structure when cultured on a supporting substrate [13]. Several assays have modeled angiogenesis *in vitro*, including the short-term culture of endothelial cells on Matrigel, a gelatinous protein mixture obtained from Engelbreth-Holm-Swarm mouse sarcoma cells [14]. This Matrigel assay is quick and easy to perform and allows *in vitro* modeling of endothelial cell behavior, including survival, apoptosis, and the steps leading to capillary formation and invasion. It is also important to investigate the effects of drugs or small molecules on angiogenesis *in vitro* before they are developed into clinical therapies.

In this study, we performed the Matrigel assay to evaluate the tubulogenic capacity of ADMSCs and UCBMSCs and compared them to hUVECs'. As shown in Figure 4, hUVECs started to change the morphology and rearranged the cell distribution at 4h. The tube-like structure was maintained until the end of the observation (8h). Meanwhile, ADMSCs changed their morphology into a tube-like structure network earlier (2h). However, this network was then quickly restructured, and the cell turned into a round shape following the observation time. The tube-like structure network completely disappeared at 8h. A similar observation was obtained for UCBMSCs (Figure 4A). Fluorescence images clearly expressed the difference in the tube formation between the three cell types (Figure 4B).

We used Image J software to analyze the total tube length, the number of meshes, the total meshes area, and the mean mesh size (Figure 5A). Quantitatively evaluation of the three cell types' angiogenic capacity indicated that both types of MSCs were not able to maintain the tube formation capacity at the time point of 6h, with all the values of the total tube length, the number of meshes, the total meshes area, and the mean mesh size was much smaller than the control ($p<0.0001$) (Figure 5B).

A previous study by Liem et al. indicated that a UCBMSC-conditioned medium could induce the tube formation of hUVECs through the secretion of some growth factors such as VEGF-A, HGF, and FGF [10]. The ADMSC-conditioned medium was also reported to secret these growth factors [15]. Hence, we would like to check if these MSCs could form the tube themselves in this study. The data showed that UCBMSCs and ADMSCs could form the tube early but rapidly restructured. This could be due to the decrease of growth factors over time, so the cells could not maintain their tube-like structure. In further works, we will add growth factors by the time of the experiment to check in this could rescue the angiogenic ability of these MSCs. Furthermore, we will check the differentiation capacity of these MSCs into endothelial cells in vitro.

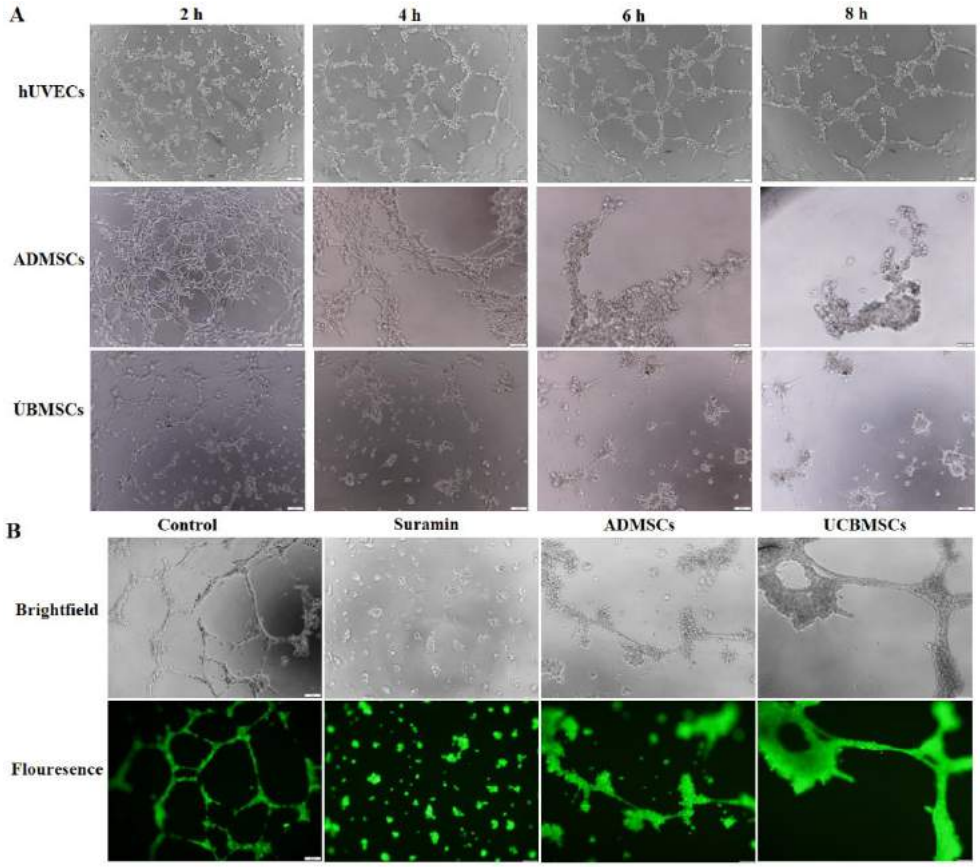

Figure 4. The tube-formation morphology of ADMSCs and UCBMSCs. (A) The formation of tubes was followed by indicated time in each cell type. (B) The formation of the tubes at the time point of 6h in brightfield and fluorescence observation

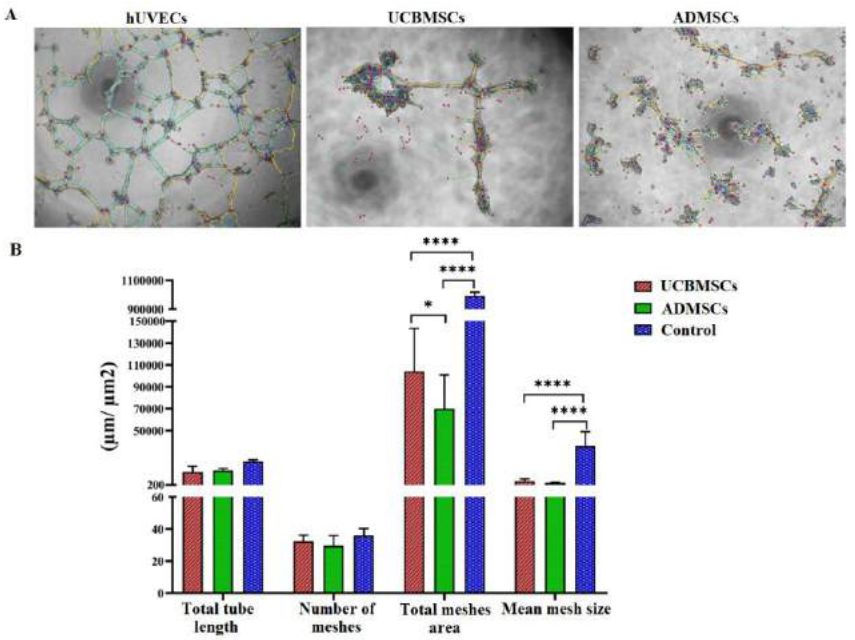

Figure 5. Quantitative analysis of tube formation capacity in ADMSCs and UCBMSCs. (A) The Image J software analysis each image of different cell types. (B) Quantitative comparison of tube-formation capacity in three cell types. *p<0.05; ****p<0.0001. Data were presented as mean ± SD (n=3).

Acknowledgment

This research was supported by the Vingroup Innovation Foundation, code: VINIF.2020.DA07.

REFERENCES

1. **Jahani, M., Rezazadeh, D., et al. (2020)**. Regenerative medicine and angiogenesis; challenges and opportunities. Adv Pharm Bull, 10 (4), pp 490-501.
2. **Tímár, J., Döme, B., et al. (2001).** Angiogenesis-dependent diseases and angiogenesis therapy. Pathol Oncol Res, 7 (2), pp 85-94.
3. **Tao, H., Han, Z., et al. (2016).** Proangiogenic features of mesenchymal stem cells and their therapeutic applications. Stem Cells Int, 2016, pp 1314709.
4. **Watt, S.M., Gullo, F., et al. (2013).** Proangiogenic features of mesenchymal stem cells and their therapeutic applications. Br Med Bull, 108 (1), pp 25-53.
5. **Crisan, M., Corselli, M., et al. (2012).** Perivascular cells for regenerative medicine. J Cell Mol Med, 16, pp 2851–60.
6. **Ding, L., Morrison, S.J. (2013).** Haematopoietic stem cells and early lymphoid progenitors occupy distinct bone marrow niches. Nature, 495, pp 231–35.
7. **Bagley, R.G., Weber, W., et al. (2009).** Human mesenchymal stem cells from bone marrow express tumor endothelial and stromal markers. Int J Oncol, 34 (3), pp 619-27.
8. **Amati, E., Sella, S., et al. (2017).** Generation of mesenchymal stromal cells from cord blood: evaluation of in vitro quality parameters prior to clinical use. Stem Cell Res Ther, **8** (14)
9. **Tsuji, W., Rubin, J.P., Marra, K.G. et al. (2014).** Adipose-derived stem cells: Implications in tissue regeneration. World J Stem Cells, 6 (3), pp 312-21.
10. **Nguyen, L.T., Tran, N.T., Than, U.T.T. et al. (2022)**. Optimization of human umbilical cord blood-derived mesenchymal stem cell isolation and culture methods in serum- and xeno-free conditions. Stem Cell Res Ther, **13** (15).
11. **Dominici, M., Le Blanc, K., et al. (2006).** Minimal criteria for defining multipotent mesenchymal stromal cells. Cytotherapy, 8 (4), pp 315–7.
12. **Goncharov, N.V., Nadeev, A.D., et al. (2017).** Markers and biomarkers of endothelium: when something is rotten in the state. Oxid Med Cell Longev. 2017, pp 9759735.
13. **Ucuzian, A.A., Greisler, H.P. (2007).** In vitro models of angiogenesis. World J Surg, 31 (4), pp 654-63.
14. **Benelli, R., Albini, A. (1999).** In vitro models of angiogenesis: the use of Matrigel. Int J Biol Markers, 14 (4), pp 243-6.
15. **Matsuda, K., Katrina, J., et al. (2013).** Adipose-derived stem cells promote angiogenesis and tissue formation for in vivo tissue engineering. Tissue Engineering Part A, 19 (11-12), pp 1327-1335.

CHANGES IN URINARY CELLS IN EXPERIMENTAL HEATSTROKE IN RABBITS

Cao Hong Phuc[1], Vu Quang Phong[1], Do Ngoc Hop[1], Nguyen Thi Thu Hien[1]

ABSTRACT

Objective: *Describing the changes in rabbit's urinary cells in experimental heatstroke rabbits.* ***Methods:*** *experimenting on the 23 rabbits, protocol: temperature 42^{0}C, humid 60%, time 2,5 hours, indexes: urinary erythrocytes, leukocytes, survival time, core temperature.* ***Results:*** *the rate of urinary erythrocyte rabbits increased, about 82.6% at 60 min, 65,2% at 24 hours after heatstroke meanwhile it was 0% before heatstroke (0%). The rate of urinary leukocyte rabbits was 0%. The grade of urinary erythrocyte did not relate to clinical grade, core temperature, and survival time.* ***Conclusion:*** *there were the urinary erythrocyte but not urinary leukocyte in experimental heatstroke.*

Keywords: *urinary erythrocyte, urinary leukocyte, heatstroke.*

1. INTRODUTION

Heatstroke is a clinical disorder that has a collapse of central neurological function and hyperthermia (over 40^{0}C) [5], [2]. The patients might die due to severe functional disorders. They may die not only due to out-hospital but also in-hospital ones. Some researchers indicated that the death ratio was about 70% of heatstroke patients in ICU and hospital [6]. If the patients were diagnosed and given emergency early, they can survive. Therefore a quick test that can support to early diagnosis and the prognosis is necessary for clinical.

Heatstroke-induced kidney injury was remarked plentifully but most previous studies only evaluated the changes in plasma components [8], [9], [10]. There have been few of them which have focused on urinary changes. The urine was the production of kidney function so the urinary changes can reflex the kidney injuries, especially the urinary cells.

[1]Military Medical University
Main author and correspondant:
Cao Hong Phuc
Email: yenlamphuc@vmmu.edu.vn
Recieved date: 19/7/2021
Reviewed date: 28/7/2021
Accepted date: 15/9/2022

Normally, the urinary cells were not appeared. When the kidney glomerulus, tube, or urinary system tracts are injured, the cells will be appeared. The discovery of urinary cells is a cheap, easy, quick test in clinical. It might be useful to apply to clinical heatstroke. *To discover the kidney injury and find out a quick test to diagnose the heatstroke, this study was performed to describe the changes in urinary cells in experimental heatstroke.*

2. METHODS

2.1. Subjects

The animals were 23 New Zealand White rabbits, weighted 2.2 – 2.5kg, randomly sex, were supplied by Bavi Rabbit Company. All animals were transferred to experimental area 3 days before studying. The conditions were: plentiful food, environment temperature 25 – 28^{0}C, the light cycle 12/12

The inclusion criteria: healthy, enough weight, did not get the gastrointestinal, respiratory, neurological, and movement diseases. The rabbit which had at least one of that symptoms was excluded.

2.2. Methods

* Study design: a prospective, experimental study, comparing the data between before and after heatstroke.

*Rabbit heatstroke model

The heatstroke model in this study was the same as our previous study [4]: the condition in chamber VK21: chamber temperature 42^0C, humidity 60%, wind speed 1 m/s, 2.5 hours. The heatstroke criteria in rabbits were similar to criteria of Shih (1984), Tong (1996) and our previous studies [12], [13], [4], including: awareness decrease, reduced mobility, paralysis of at least one leg, supine test (+), convulsions, death within 60 minutes after heatstroke (AH), rectal temperature at least 42^0C.

Based on clinical symptoms, we divided the heatstroke into 2 grades: mild when rabbits did not die; severe when rabbits were convulsed and died within 60 minutes AH.

*Sampling method

The sample was urine. Urine was collected using a catheter, ø 1mm, inserted directly into the rabbit bladder. Collecting all of the urine from the bladder (the urine stops coming out). Then, tested by the Combostik R-300 semi-automatic urine testing instrument (DFI Company, Korea). Sampling time: 24 hours before heatstroke (BH), 60 minutes, 24 hours AH.

* Research indicators

-The erythrocyte count and leukocyte count in the urine: expressed as levels 0, 1+, 2+, 3+.

-Survival time: calculated from heatstroke to 24 hours AH (minutes).

2.3. Data analysis

Data are expressed as a count (n), a percentage (%), minutes. Comparing the difference between the points of time of study, clinical grades, urinary cell grades, Chi-square test was used, the difference was determined with $p<0.05$.

3. RESULTS

The changes of urinary cells are presented in tables 1 - 3 and chart 1. The results showed that, in AH, rabbits had more red blood cells in urine and more severe than before heatstroke (BH). Urinary erythrocyte grade at the time of 60 minutes, 24 hours AH was different from BH, $p<0.01$ (Table 1). Thus, after suffering from experimental heatstroke, rabbits showed red blood cells in the urine, which was different from before one. Similarly, we observed the appearance of leukocytes in urine and found out no leukocytes in the urine (Table 2). The leukocyte status AH remained the same as that of BH.

In order to evaluate the clinical value of the urinary red blood cell, we investigated the relation of this index to clinical grade, survival time, and core temperature. Table 3 shows that the level of urinary red blood cells at the time of 60 minutes AH is similar between mild and severe clinical grade. At this point, there were mainly grade 1+ erythrocytosis which appeared in urine, the rate of mild and severe rabbits was 58.3 and 63.6%, respectively. There is no difference in urinary erythrocyte rate or grade at 60 minutes AH. The results were low value in predicting the clinical severity. Surveying the survival time, chart 1 shows that the survival time of rabbits with severe urinary erythrocytosis tended to be shortened but not statistically significant. Urine erythrocyte at 60 minutes AH has little predictive value in survival ability.

In terms of core temperature, we did not notice a difference in the degree of urinary erythrocyte with the core temperature (Figure 1).

Table 1. Change of urinary erythrocyte in heatstroke

Level Urinary erythrocyte	24 hours BH n (%)	60 minutes AH n (%)	24 hours AH n (%)
Grade 0	23 (100)	4 (17.4)	8 (34.8)
Grade 1+	0 (0)	14 (60.9)	1 (4.3)
Grade 2+	0 (0)	2 (8.7)	2 (8.7)
Grade 3+	0 (0)	3 (13.0)	1 (4.3)
Total	23 (100)	23 (100)	12 (100)
p	<0.01		

Table 2. Change of Urinary leukocyte in heatstroke

Level Urinary leukocyte	24 hours BH n (%)	60 minutes AH n (%)	24 hours AH n (%)
Grade 0	23 (100)	23 (100)	12 (100)
Grade 1+	0 (0)	0 (0)	0 (0)
Grade 2+	0 (0)	0 (0)	0 (0)
Total	23 (100)	23 (100)	12 (100)
p	X		

Table 3. The relationship between urinary erythrocyte at 60 minutes AH with disease severity

Level Urinary leukocyte	Mild grade n (%)	Severe grade n (%)	p
Grade 0	2 (16.7)	2 (18.2)	>0.05
Grade 1+	7 (58.3)	7 (63.6)	
Grade 2+	2 (16.7)	0 (0)	
Grade 3+	1 (8.3)	2 (18.2)	
Total	12 (100)	11 (100)	

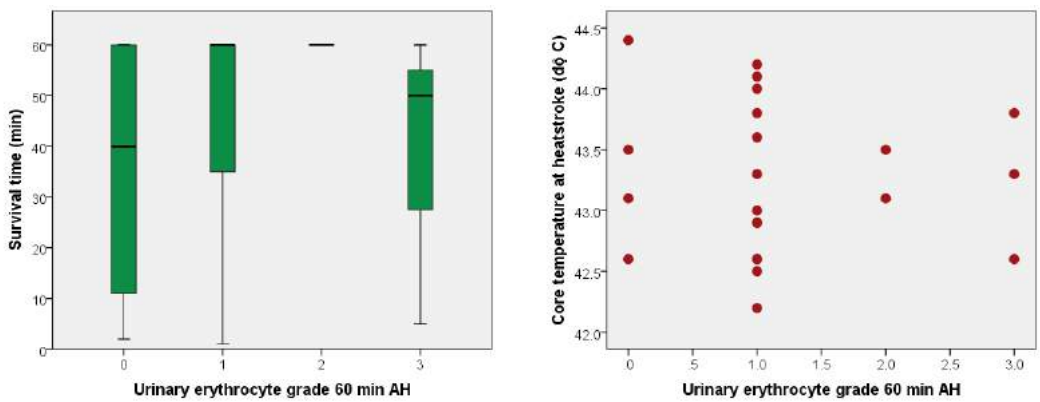

Figure 1. The relationship between urinary erythrocytes at 60 minutes AH with survival time and core temperature

(The urinary erythrocyte grade was not associated with survival time and core temperature)

4. DISCUSSION

The kidneys and urinary system are an endogenous system for eliminating toxins from the body. The elimination mechanism is plasma ultrafiltration that allows only small soluble components to be filtered. The large soluble components (>500 kDa) or cellular components are retained and cannot be eliminated. Therefore, there are no cells in the urine [6], [3]. Another important respect, urine is a direct product of renal function, so the urinary test can detect some microscopic damage in the kidneys and urinary system [2].

Table 1 showed that BH urinary erythrocyte was almost absent but it was present AH. The percentage of rabbits with red blood cells in urine increased, reaching 82.6% at the time of 60 minutes AH while the BH rate was 0%. Similarly, at 24 hours AH, the percentage of rabbits with red blood cells in urine reached 65.2%. The difference in the percentage of urinary erythrocyte rabbits was statistically significant. The degree of erythrocyte also appeared to be different at different time points of the study. These results led to the observation that a symptom of experimental heatstroke is urinary erythrocyte. This observation is clinically useful when examining the atypical heatstroke patients and demonstrating kidney and urinary system damage when rabbits have experimental heatstroke. Red blood cells can be filtered at two injured locations: the ultrafiltration membrane in the glomerular and the basement membrane in the renal tubes [6], [3]. In this study, we did not have enough data to determine the location of the lesion, but it confirmed that there might be a lesion in the above locations.

This damage is mainly caused by heat, not inflammation. Table 2 showed no urinary leukocytes. Thus, cell damage in the urinary tract is not caused by an inflammatory response. We were quite surprised by this result, although, in principle, every injured cell could trigger an inflammatory response. The leukocytes did not extravasate, penetrate, or pass through the lesion to pass from the blood into the urinary tract. The mechanism of the absence of leukocytes needs further investigation.

Urinary cell damage is caused by some mechanisms: heat, circulatory decrease, and/or oxidative stress [5], [8], [10]. In order to investigate the mechanism of heat injury, we monitored the degree of hyperthermia and the level of red blood cells in the urine. Chart 1 shows no such correlation. Thus, the temperature is not the main factor causing urinary tract cell damage. The highest core temperature was at not only urinary erythrocyte level 2+, 3+ but also level 0 and 1+. Apparently, high core temperature was not the main cause of erythrocytosis, although its role could not be ruled out.

The urinary test is cheap, common, and easy to perform. Therefore, it is expected that the test contributes to the prognosis of clinical grade or survival time. Table 3 shows that the contribution of urinary erythrocyte in prognosis the clinical grade was low, there is no difference in the level of erythrocytes between clinical severity. The distribution of urinary erythrocytes status was similar between mild and severe disease ($p>0.05$). Thus, the severity of the disease depends on something other than the urinary tract (and therefore the erythrocytosis). Figure 1 also shows that the urinary erythrocyte value has little significance in predicting survival time. A rabbit which has severe erythrocytosis, much urinary tract damage might live longer than rabbits with mild erythrocytosis, little urinary tract damage. The survival time of rabbits may depend on other factors [9],[10], [11].

5. CONCLUSION

From the research results, we draw the conclusion: there are urinary

erythrocytes but no leukocyte in experimental heatstroke. The urinary red blood cell grade was not associated with clinical severity, core temperature, and survival time.

Suggestions

Further research is needed on kidney damage and the mechanism of urinary tract cell damage in heatstroke.

Acknowledgement

We thank the Fundamental Research Fund (Military Medical University) for sponsor this research. We also thank the Department of Military Occupational Medicine (Military Medical University) for technical and material support for this study.

REFERENCES

1. **Học viện Quân y (2007),** Sinh lý học, Giáo trình giảng dạy đại học. Tập 1. NXB. Quân đội Nhân dân, Hà Nội, tr. 342-355.
2. **Học viện Quân y (2017),** Sinh lý lao động quân sự. NXB. Quân đội Nhân dân, Hà Nội, tr. 133-145.
3. **Học viện Quân y (2019),** Hóa sinh y học, Giáo trình giảng dạy đại học và sau đại học. NXB. Quân đội Nhân dân. Hà Nội, tr. 265-301.
4. **Vũ Quang Phong, Bùi Duy Hoàn, Đỗ Ngọc Hợp, Nguyễn Văn Tuân, Nguyễn Văn Tiến, Lang Minh Thiên, Nguyễn Việt Anh, Đỗ Việt Vương, Cao Hồng Phúc (2020),** Nghiên cứu sự biến đổi điện tim và cơ chế mô bệnh cơ tim trên mô hình thỏ say nóng thực nghiệm, TC Sinh lý học Việt Nam, 24(4), 7-14.
5. **Hall JE (2016),** Guyton and Hall Textbook of Medical Physiology, Jordanian Edition E-Book. Elsevier.
6. **Hifumi T, Kondo Y, Shimizu K, Miyake Y (2018),** Heat stroke. Journal of intensive care. 6(1):1-8.
7. **Knochel JP, Beisel WR, Herndon Jr EG, Gerard ES, Barry KG (1961),** The renal, cardiovascular, hematologic and serum electrolyte abnormalities of heat stroke. The American journal of medicine. 30(2):299-309.
8. **Lumlertgul D, Chuaychoo B, Thitiarchakul S, Srimahachota S, Sangchun K, Keoplung M (1992),** Heat stroke-induced multiple organ failure. Renal failure. 14(1):77-80.
9. **Nabalawi RA (2011),** Renal and electrolyte abnormalities in heat stroke during Hajj. Saudi Journal of Internal Medicine. 1(2):33-35.
10. **Sato Y, Roncal-Jimenez CA, Andres-Hernando A, Jensen T, Tolan DR, Sanchez-Lozada LG, Newman LS, Butler-Dawson J, Sorensen C, Glaser J (2019),** Increase of core temperature affected the progression of kidney injury by repeated heat stress exposure. American Journal of Physiology-Renal Physiology. 317(5):F1111-F1121.
11. **Shih CJ, Lin MT, Tsai SH (1984),** Experimental study on the pathogenesis of heat stroke. Journal of neurosurgery. 60(6):1246-1252.
12. **Tong ZF, Jun ZH, Zhi QR, Jun LW, Chu HX (1996),** Experimental study n induced heat stroke in rabbits [Japanese]. Chinese Journal Of Pathophysiology. 4.
13. **Trujillo MH, Fragachán GC (2011),** Rhabdomyolysis and acute kidney injury due to severe heat stroke. Case reports in critical care. 2011.

DEVELOPMENT OF ALLERGEN EXTRACTION METHOD IN PEEL AND PULP OF FRESH TOMATOESTHAT CAUSE ALLERGY IN HUMAN

Phan Thi Tuyet Nhung[1], Hoang Khanh Hang[1], Nguyen Thi Thuy Hang[1], Nguyen Dinh Duyet[1], Phan Thi Minh Phuong[2], Grazia Galleri[3]

SUMMARY

Background: *Tomatoallergens have been extensively studied but the simple and advanced extraction method from peel and pulp of fresh tomatoes has yet to be performed.* ***Objects:*** *To develop the proteinextraction method fromtomato peel and pulp and to investigate the allergenicity of the tomato peel and pulp extracts.****Methods:*** *Applying two different protocols and SDS-PAGE for extracting allergens from the peel and pulp of fresh tomato and performing immunoblotting them with sera of 9 allergic patients with tomato.* ***Results:*** *The samples extracted by thesecond protocol showed clearer and more bands than thoseby the first protocol. The immune reaction measured by Immunoblotting analysis with tomatopeel extracts exhibited more specific and visualized bands on membranes compared with those from pulp extracts. In detail, most of allergic patients to tomato reacted with peel's allergens such as Profilin and Sola I5 Cyclophilin.* ***Conclusion:*** *Confirm thatthe second protocol in this research can be considered as the effective method for proteinextractionfrom freshtomato peel and pulp; and the main cause of tomato allergy comes from tomato's peel.*

Keywords: *allergens, SDS-PAGE, immunoblot, silver staining.*

1. INTRODUCTION

Food allergy has become a serious health concern that affects children and adults. The prevalence of food allergy is rising for unclear reasons, with prevalence estimates in the developed world approaching 10%. [1] Food-induced allergic reactions can be attributed to IgE-mediated and non–IgE-mediated (cellular) mechanisms [2]. Nevertheless, food allergy is primarily IgE antibody mediated and thus, classified as an allergy of the immediate type or Type-I-hypersensitivity.

[1]Department of Physiology, Hue University of Medicine and Pharmacy
[2]Department of Immunology and Pathophysiology, Hue University of Medicine and Pharmacy
[3]Department of immunology experiment and flow cytometry, Sassari University, Italy
Corresponding author: **Phan Thi Tuyet Nhung**
Email: pttnhung@huemed-univ.edu.vn
Receptived date: 25/7/2021
Reviewed dated: 03/8/2021
Accepted date: 15/9/2022

Tomatoes are a major component of diets around the world and thus are intensively consumed. In recent publications, tomato has been confirmed as one of the most prevalentplant-derived food sensitizer [3], [4] with an allergenic frequency that ranges between 1.5 and 20.0% in different populations of patients with specific IgE [5], [6]. The prevalence of tomato allergy ranges from 1.5% in northern Europe [7] up to 16% in Italy [8] among the food-allergic population.

Up to now, several tomato allergens have been identified and characterized in fresh tomato fruit, in particular, Lyc e 1 [9], [10], Lyc e 2 of 50 kDa[11] and Lyc e 3 of 9 kDa [12]… by different methods in some clinical studies.These allergens may come from each parts of tomato including peel, pulp, seed. After reviewing lots of documents and studies focusing on how to extract tomato allergens, we realised these methods were too complicated and need some unavailable chemicals. Therefore, an advanced way for tomato extraction was

necessary. Moreover, each tomato component is probably well- recognized as potent inducer for allergy, so it needs to investigate the allergenic potency from different part of tomato by immunoreaction between them and allergic subjects. In the context of tomato allergy, we conducted a research "*Development of allergens extraction method in peel and pulp from fresh tomatoes that cause allergy in human".*

The aims of this study were to develop the proteinextraction method fromtomato peel and pulp and to investigate the allergenicity of these extracts.

2. MATERIALS AND METHODS:

2.1. Allergenic source preparation

Two fresh, ripe tomatoes (Grappolo) in optimal conditions for human consumption were purchased in the supermarket and weigh about 154 gram, 170 gram and stored at 4^0C until using for analysis. Before extraction, they were washed in distilled water and carefully manually separated into different parts: peel, pulp, seed moisture by using knife and put these parts into Falcon tubes. Peel is the skin of tomato while pulp is the reddish meat once discarded peel, seeds and the things covered around the seeds is seed moistures.

2.2. Patients

Nine patients in this study had clinical history with tomato allergy judged by fluorescence enzyme immunoassay (FEIA) tests at hospital of Sassari University. After obtaining informed consent, sera were taken from all patients and stored at -20^0C until used.

The Ethics Committee approved the studyand all selected patients were enrolled after providing their informed consent.

2.3. Methods

2.3.1. Allergen extraction procedures

Applying two different protocols and SDS-PAGE for extracting allergens from the peel and pulp of fresh tomatoes:

Protocol 1: The peel and pulp of fresh tomato were separately homogenized in physiological saline 0.9% (2:1/w: v) and inhibitor protein (mini complet with EDTA 7X :1 tablet) by using Ultra-Turrax T25 (Janke & KunKel IKA-Labortechnik) 30 seconds x8 times with ice bath. All two homogenates were put in conical glasses and left continuous magnetic stirring in ice bath for 4 hours. Then the extracts were precipitated with prechilled acetone (v:v/1:2). When performing SDS-PAGE, the concentration of sample loaded into each well was 50.8µg of pulp, 150µg of peel. The extracts were separated by 4% stacking gel and 12% running gel polyacrylamide including 6% glycerol.After finishing electrophoresis, the gel was stained with a blue dye called Coomassie Brilliant Blue r-250 (CBB) (Methanol 40%, Acid acetic 10%, Coomassie 0.1% and Deionized water) for 15 minutes and then washed with destaining solution five times. Then, the separation of proteins with different molecular weights was shown by comparison with a mixture of standard proteins.

Protocol 2: Each part of tomato was extracted with the similar steps to the first one but it was changed with some solution and volume… In particular, the different parts were separately homogenized in PBS 1X pH 7.3 (w: v/1:5, except the pulp w: v/2:1) by using Ultra-Turrax T25/ 30 seconds x 20 times with ice bath. Then the extracts were precipitated with prechilled acetone (v: v/1:2). For the electrophoresis, the concentration of protein in each well was 600µg that were increased in comparison with the first protocol. The extracts were separated by both 4% stacking gel and 15% running gel polyacrylamide without 6% glycerol.After finishing electrophoresis, the gel was stained with a blue dye called Coomassie

Brilliant Blue r-250 (CBB) (Methanol 40%, Acid acetic 10%, Coomassie 0.1% and Deionized water) for 15 minutes and then washed with destaining solution five times. Then, the separation of proteins with different molecular weights was shown by comparison with a mixture of standard proteins.

2.3.2. Immunoblotting

After confirming the protocol 2 as the improved procedure for peel and pulp extraction method, we decided to investigate the allergenic tomato components(peel and pulp) separated by the second one when immunoblotting with patients 'sera. The detailed process was as follows:

- Using peel and pulp extraction from the second method, the two gels were transferred onto 2 nitrocellulose papers by electroblotting. The remaining gel was transferred to Hoefer SE300 miniVE system by using the nitrocellulose sheet (GE Healthcare Bio-Sciences, LittleChalfont, UK).

- The sera from 9 patientswith 1:10 dilution was incubatedwith peel and pulp samples on membranes.The images were obtained from incubations with the sera of subjects in this dilution and then with secondary antibody IgE antibodies – alkaline phosphatase conjugate (Invitrogen) diluted 1:2000. The immuno complex were diagnosed by using BCIP/NBT Substrate Solution, which contains BCIP (0.15 mg/ml), NBT (0.30 mg/ml), Tris buffer (100 mM), and MgCl2 (5mM), pH 9.25- 9.75.

3. RESULTS

3.1. The first protocol

Pulp and peel extracts taken from -20^{0}C were used for separation by SDS-PAGE. Figure 1 showed the samples separated by the first protocol (12% running gel with 6% glycerol) appeared a few non- clear bands.

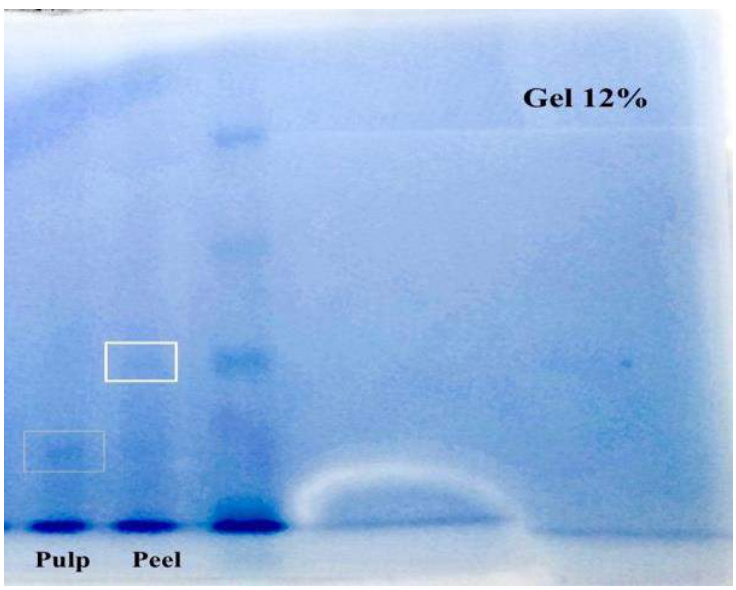

Figure 1. SDS- PAGE using 12% running gel with 6% glycerol

3.2. The second protocol

The developed protocol for extraction was applied with some alternatives, specially using 15% running gel without 6% glycerol. After SDS PAGE, the gel was not only stained with Coomassie Blue (Figure 2) but also with sensitive way (Figure 3), so that lots of bands were clearly identified.

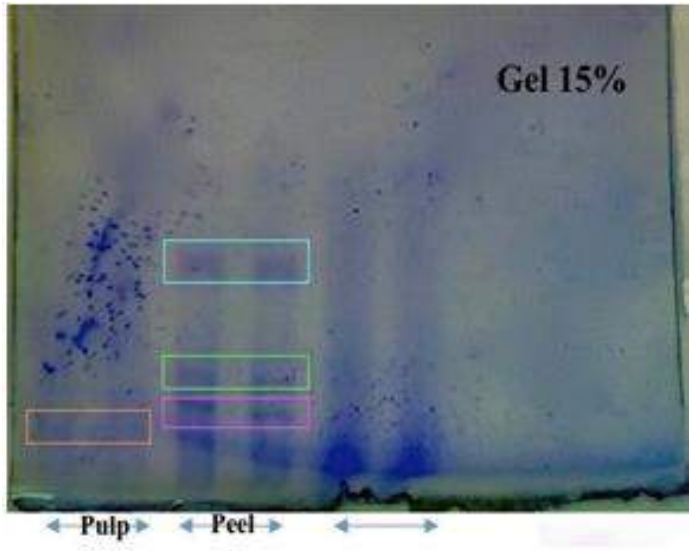

Figure 2. SDS- PAGE using 15%running gelwithout 6% glycerol

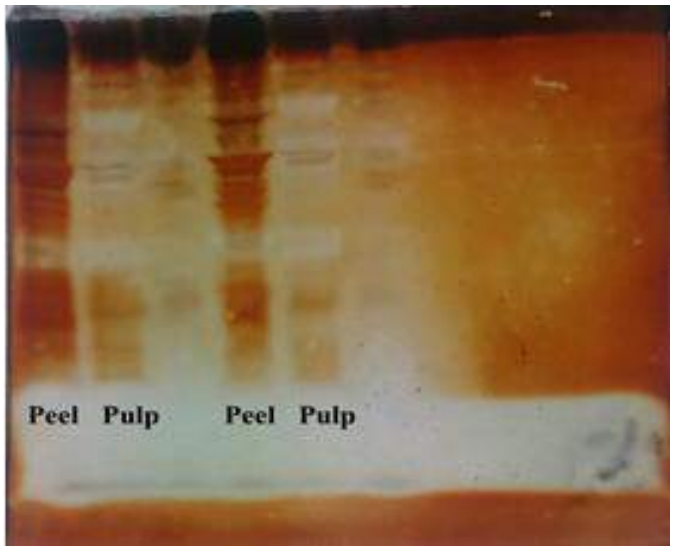

Figure 3. SDS- PAGE using 15% running gelwithout 6% glycerol and silver staining

3.3 Immunoblotting

Immunoblotting analysis of peel extract (figure 4) showed that a lot of bands visualized on membranes of the 1st, 3th, 4th, 5th, 6th, 7th and 8th subject. In addition, a lot of patients reacted with the same peel allergen, for instance, the 14kDa band (Profilin) detected in sera of 3th, 4th and 6th subject, Sola I5 Cyclophilin tomato allergen (with molecular weight of 19kDa) appeared in both 1st and 7th serum.

Every serum sample reacted with pulp molecules. However, serum of the 4th patient had the strongest reaction in which 2 clear band can be observed at position of 55kDa and 45kDa, that were respectivelycharacterisedas Lyc e Glucanase and Lyc e Peroxidase.

4. DISCUSSION

4.1. Identify the effective protocol for allergen extraction from fresh tomatoes

Up to now, several tomato allergens have been extracted and characterised by

a lot of procedures. These tomato allergens come from different parts such as peel, pulp, seed. Numerous publications have presented lots of complex extraction methods, so that the primary end point of the study was the evaluation and comparison of the two techniques for confirming the developed extraction protocol in tomato's peel and pulp.We tried to apply two simpler methods based on these references: "Detection of a novel Allergen in raw Tomato"," Two nonspecific lipid transfer proteins (nsLTPs) from tomato seeds are associated to severe symptoms of tomato-allergic patients".

A few bands were obtained on gel separated by the protocol 1. It can be realized that the mobility of molecules in electric field of 12% running gelwere too fast so that not too many bands appeared and they were at the lower part of the gels or we might lose some bands during the migration. Some reasons can explain for these events:

+ The presence of glycerol and the magnitude of the applied field that was not complicated enough made molecules migrate

+ The concentration of samples was too little for separation

+ Too much time for migration

Next, we modified protocol with some alternatives as the second one: higher concentration of running gel (15% instead of 12%) without 6%glycerol, increasing sample concentration and reducing time for separation (3 hours 30 minutes). Actually, clearer and more bands of peel and pulp were obtained on gel (15% running gel without 6%glycerol) when using this developement extraction method (Figure 2). It has been realized after changing some details in the protocols that the improved procedure was suitable with peel and pulp extraction. Therefore, we confirmed this procedure for the next analysing processes as well as the developed protocol for allergen extraction from fresh tomato.

4.2 Determine the main cause of tomato allergy coming from the peel allergens

Each allergic subject to tomato expresses different symptoms, so we hypothesized that each subject reacts with different allergens from tomato's peel or pulp. On these basis concepts, we decided to investigate IgE reactivity of the single part of tomato (peel, pulp) with 1:10 diluted serum of every allergic patientwith tomato, which helps to detect the main allergic reason coming from either peel or pulp.

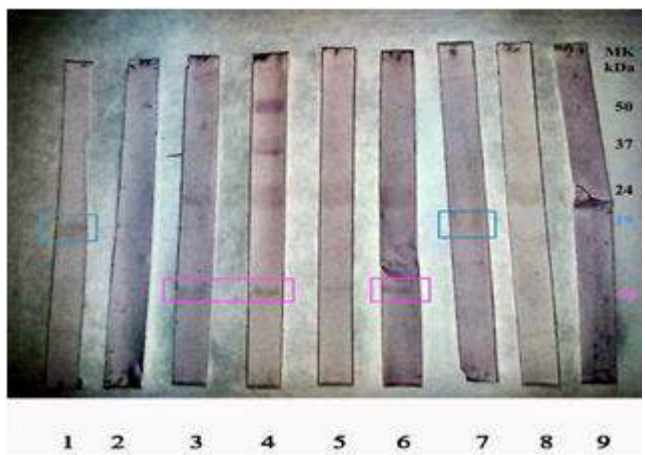

Figure 4. Immunoblotting of peel extract with9 sera from allergic patients with tomato

Figure 5. Immunoblotting of pulp extract with 9 sera from allergic patients with tomato

It can be seen that most of allergic patients occurred the immune response with peel extract, which was proved by the appearance of many bands visualized on membranes of seven patients. On the other hand, the only 4thpatientappeared the reaction between pulp allergen and specific IgE.

Another realization was that a number of reactive bands in peel were more than in pulp, which indicated most of subjects reacted with the peel allergens. Consequently, the allergens in all these subjects mostly originate from the peel.

Some allergens found in other studies have cross-reaction with others. For instance, tomato skin/flesh profilins will cause only a mild reaction and you may cross-react withpeppers and grass pollen.Also, the involvement of the allergenic nonspecific lipid transfer proteins from tomato fruit in cross- reactivity processes with other vegetables foods such as fruits from Rosaceae family, or even a material like latex, adds more complexity to the diagnosis of this food allergy[13].

5. CONCLUSION

In our study, two protocols for tomato extraction were presented and applied. These two procedures were referred from a number of publications and adjusted some details based on available conditions. After comparing the results that analysed by SDS-PAGE, we confirmed the second one as an effective protocol for extraction and characterisation.

Our findings showed that thesera of patients mostly reacted with the allergens of peel, hence the main cause of tomato allergy comes from tomato's peel.

Acknowledgements

The authors sincerely thank all the staffs at laboratory of immunology experiment and flow cytometry in Sassari university for facilitating us to conduct our study.

REFERENCES

1. **J. Savage and C. B. Johns (2015)**, "Food Allergy : Epidemiology and Natural History," *Immunol Allergy Clin North Am*, vol. 35, no. 1, pp. 45–59.
2. **H.A Sampson *et al.* (2014**), "Food allergy: A practice parameter update-2014", J*. Allergy Clin. Immunol.*, vol. 134, no. 5, p. 1016-1025.e43.
3. **O. Y. Bässler *et al.* (Mar. 2009***)***, "Evidence for Novel Tomato Seed Allergens: IgE-Reactive Legumin and Vicilin Proteins Identified by Multidimensional Protein Fractionation−Mass Spectrometry and in Silico Epitope Modeling," *J. Proteome Res.*, vol. 8, no. 3, pp. 1111–1122.

4. **C. H. Larramendi *et al.* (2008)**, “Sensitization to tomato peel and pulp extracts in the Mediterranean Coast of Spain: Prevalence and co-sensitization with aeroallergens,” *Clin. Exp. Allergy*, vol. 38, no. 1, pp. 169–177.
5. **B. K. Ballmer-Weber and K. Hoffmann-Sommergruber (2011)**, “Molecular diagnosis of fruit and vegetable allergy,” *Current Opinion in Allergy and Clinical Immunology*, vol. 11, no. 3. pp. 229–235.
6. **M. Geroldinger-Simic *et al.* (2011)**, “Birch pollen-related food allergy: Clinical aspects and the role of allergen-specific IgE and IgG4antibodies,” *J. Allergy Clin. Immunol.*, vol. 127, no. 3, 616–622.
7. **A. Petersen, S. Vieths, H. Aulepp, M. Schlaak, and W. M. Becker (1996)**, “Ubiquitous structures responsible for IgE cross-reactivity between tomato fruit and grass pollen allergens,” *J. Allergy Clin. Immunol.*, vol. 98, no. 4, pp. 805–815.
8. **C. Ortolani, M. Ispano, E. A. Pastorello, R. Ansaloni, and G. C. Magri (1989)**, “Comparison of results of skin prick tests (with fresh foods and commercial food extracts) and RAST in 100 patients with oral allergy syndrome,” *J. Allergy Clin. Immunol.*, vol. 83, no. 3, pp. 683–690.
9. **M. Willerroider *et al.* (2003)**, “Cloning and molecular and immunological characterisation of two new food allergens, Cap a 2 and Lyc e 1, profilins from bell pepper (Capsicum annuum) and tomato (Lycopersicon esculentum),” *Int. Arch. Allergy Immunol.*, vol. 131, no. 4, pp. 245–255.
10. **S. Westphal, W. Kempf, K. Foetisch, M. Retzek, S. Vieths, and S. Scheurer (2004**), “Tomato profilin Lyc e 1: IgE cross-reactivity and allergenic potency,” *Allergy Eur. J. Allergy Clin. Immunol.*, vol. 59, no. 5, pp. 526–532.
11. **S. Westphal *et al.* (2003)**, “Molecular characterization and allergenic activity of Lyc e 2 (β-fructofuranosidase), a glycosylated allergen of tomato,” *Eur. J. Biochem.*, vol. 270, no. 6, pp. 1327–1337.
12. **K. Foetisch *et al.* (2001**), “Tomato (Lycopersicon esculentum) allergens in pollen-allergic patients”,*Eur. Food Res. Technol.*, vol. 213, no. 4–5, pp. 259–266.
13. **Laura Martin- Pedraza et al.(2016)**, “Two nonspecific lipid transfer proteins (nsLTPs) from tomato seeds are associated to severe symptoms of tomato-allergic patients”, *Mol. Nutr. Food Res*, vol. 60, pp. 1172-118.

RISK FACTORS FOR DEVELOPING PNEUMONIA IN PATIENTS WITH ACUTE LEUKEMIA RECEIVING CHEMOTHERAPY

Vu Minh Phuong[1,2], Le Khanh Linh[3], Duong Hai Yen[2]

SUMMARY

Background: *Pneumonia is one of the serious complications during chemotherapy for acute leukemia. The purpose of this study was to determine the incidence rate, clinical characteristics, and risk factors for pneumonia in patients with acute leukemia after chemotherapy.* ***Methods:*** *Two hundred and nine patients with acute myeloid leukemia (AML) and acute lymphoblastic leukemia (ALL) were enrolled in the cohort study, in which 138 patients received chemotherapy, 71 patients had previous pneumonia, so chemotherapy should be delayed.* ***Results:*** *Of the 138 patients who received chemotherapy, 40 patients (29%) developed pneumonia after chemotherapy. Post-chemotherapy pneumonia patients were less likely to have dypsnea, respiratory failure, and severity than those of previous pneumonia patients with P= 0.002, 0.004, and 0.012; respectively. Female patient, non-complete remission (CR) status (include: state of not reaching CR before or previous not received chemotherapy), neutrophil count delay below 0.5 G /L for 7 days, were risk factors for developing pneumonia after chemotherapy with P= 0.036, 0.002 and 0.005; respectively.* ***Conclusions:*** *Pneumonia after chemotherapy for acute leukemia was common. Female patients, non-CR status (include: state of not reaching CR before or previous not received chemotherapy), a delay in neutrophil count below 0.5G /L for 7 days, were high- risk factors of developing pneumonia after chemotherapy.*

Keywords: *pneumonia, leukemia, AML, ALL, chemotherapy.*

1. INTRODUCTION

Acute leukemia (include acute myelogenous leukemia (AML) and acute lymphoblastic leukemia (ALL) is group of malignant hematological diseases, characterize by anemia, leukopenia, thrombocytopenia, and profelirating of immature progenitor cell to infiltrate organs. Therefore, acute leukemia is very sensitive and susceptible to infection [1].

Of the infectious complications, pneumonia is among the most common, developing in 20 to 30% of patients undergoing induction chemotherapy for leukemia [2],[3]. Pneumonia is also one of the most serious infectious complications, with fatality rates of 16.7 to 38.5 % depending on the causative pathogen [2], [4].

The chemotherapy regimen used in the treatment of acute leukemia aims to achieve complete remission, but also causes serious complications, especially infections caused by neutropenia, including pneumonia.

Chemotherapy regimens have evolved significantly over time. Therefore, updated studies on adverse effects, including infection, as well as pneumonia, are always needed when using these regimens. Additionally, covariates that increase the risk of pneumonia, such as neutropenia, should also be considered.

The purpose of this study was to determine the incidence rate, clinical characteristics and risk factors for

[1]Hanoi Medical University
[2]Bach Mai Hospital
[3]Vietnam National Cancer Hospital
Corresponding author: Vu Minh Phuong
Email: vuminhphuong@yahoo.com
Received date: 21/4/2022
Reviewed date: 16/5/2022
Accepted date: 15/9/2022

pneumonia in patients with acute leukemia after chemotherapy.

2. METHODS

2.1. Patients

From July 2019 to July 2020, at the Center of Hematology and Blood Transfusion – Bach Mai Hospital, Hanoi, Vietnam, 209 patients confirmed AML, ALL according to the FAB classification were enrolled in our study. In which, 138 patients received chemotherapy, 71 patients had previous pneumonia, so chemotherapy should be delayed. Of these 138 patients who received chemotherapy, 40 patients developed pneumonia after chemotherapy.

2.2. Chemotherapy treatment

All 138 patients, who had not pneumonia before starting chemotherapy, accepted treatment: in which 38 patients were diagnosed for the first time and had not received chemotherapy, 66 patients who had received induction chemotherapy and achieved complete remission (CR), 13 patients had not responded to initial treatment, 21 patients had relapsed. Thirty-eight patients with new diagnosis received induction chemotherapy (Hyper CVAD course A with ALL, 3+7 regimen with AML, daunorubicin plus ATRA with APL), 66 patients with achieved CR received consolidation chemotherapy (Hyper CVAD course B with ALL, high-dose cytarabin with AML), the remaining patients (no response and relapse) received FLAG regimen.

2.3. Definitions

Definition of pneumonia on the American Thoracic Society guidelines for health care–associated pneumonia [5].

All of the following criteria were met (*1*): Chest imaging (either chest radiograph or computed tomography) consistent with pneumonia. (*2*) Temperature greater than 38.3° C (or less than 36°C), or dyspnea, or cough with purulent sputum.

Microbiologically confirmed pneumonia was defined by the isolation of a pathogen from the blood, sputum, and bronchoalveolar lavage fluid.

Assess the severity of pneumonia according to CURB 65 [6].

2.4. Statistics

Three groups were created in the statistical analysis: the pneumonia occurring after the chemotherapy group *vs.* the pneumonia occurring before the chemotherapy group, the pneumonia occuring after the chemotherapy group *vs.* the non- pneumonia after chemotherapy group. Differences in the distribution of variables between subsets of patients were analyzed using χ^2 and Fisher's exact tests. *P* -values of <0.05 were considered significant. The logistic regression model was used to analyze the associated factors. The odds ratios and respective 95% confidence intervals were estimated.

The study protocol was approved by the Ethical committee at Bach Mai Hospital, and all patients received informed consent.

3. RESULTS

3.1. Clinical data

There were 209 patients; 104 were male (M:F≡ 1.09), with an age range: 16-72 years. According to the FAB criteria, 144 patients were classified as having AML and 65 patients as ALL. The patients were grouped according to three groups: pneumonia occurring after chemotherapy, pneumonia occurring before start of chemotherapy, and non- pneumonia after chemotherapy groups (Table 1). Of the 138 patients who received chemotherapy, 40 patients (29%) developed pneumonia after chemotherapy.

Table 1. Patient characteristics according to the groups

Variable	Pneumonia occuring after chemotherapy (n=40)	Pneumonia before start of chemotherapy (n=71)	No pneumonia after chemotherapy (n=98)
Mean age (years)	46.43±15.067	58.08 ± 17.998	41.77±16.073
Sex (n/%)			
Female	25 (62.5%)	38 (53.5%)	42 (42.9%)
Male	15 (37.5%)	33 (46.5%)	56 (57.1%)
Type (n/%)			
AML	28 (70%)	58 (81.7%)	58 (59.2%)
ALL	12 (30%)	13 (18.3%)	40 (40.8%)
Response of treatment (n/%)			
Previous not received chemotherapy	20 (50%)	60 (84.5%)	18 (18.4%)
Previous received chemotherapy	20 (50%)	11 (15.5%)	80 (81.6%)
CR	11 (27.5%)	3 (4.2%)	55 (56.1%)
PR	0 (0%)	0 (0%)	0 (0%)
No response	3 (7.5%)	5 (7%)	10 (10.2%)
Relapse	6 (15%)	3 (4.2%)	15 (15.3%)

Note: Data presented are n unless otherwise indicated, CR: complete remission, PR: partial remission

3.2. Clinical features of pneumonia occuring after chemotherapy

The differences in pneumonia characteristics between pneumonia that occurs after chemotherapy and pneumonia that occurs before the start of the chemotherapy groups are presented in Table 2. Patiens with post-chemotherapy pneumonia patients were less likely to have dypsnea, respiratory failure, and severe than those with pneumonia before chemotherapy with the statistically significant difference (with *P*=0.002, 0.004, 0.012; respectively).

Table 2. Clinical characteristics of pneumonia presentations

Variable	Pneumonia occuring after chemotherapy (n=40)	Pneumonia before start of chemotherapy (n=71)	*p*	OR	95%CI
Mean age (years)	46.43±15.067	58.08 ± 17.998	**0.001**		
Cough					
Absent	0	1			
Dry cough	4	6	0.745		
Sputum cough	32	60	0.545		
Blood cough	4	4	0.456		
Fever					
Yes	39	71	0.360		
No	1	0			

Dypsnea					
No	32	36	**0.002**	**3.889**	**1.58-9.60**
Yes	8	35			
Chest pain					
No	31	59	0.470		
Yes	9	12			
Respiratory failure					
No	32	37	**0.004**	**3.676**	**1.489-9.076**
Yes	8	34			
Chest radiograph resutls					
Lobe Consolidation	1	0			
Diffuse consolidation	29	49	0.133		
Multifocal consolidation	4	16	0.114		
Interstitial opacities	4	6	0.442		
Inflammation markers					
Mean CRP hs (mg/L)	9.05±6.16	12.43±9.79	0.105		
Mean Procalcitonin (ng/mL)	1.98±4.54	3.93±12.29	0.185		
Degree of pneumonia					
Not Severe	36	49	**0.012**	**4.041**	**1.128-12.748**
Severe	4	22			

3.3. Risk factors for peumonia

There was a significant association between the post-chemotherapy pneumonia and sex (female), non-CR status (include: state of not reaching CR before or previous not received chemotherapy), a neutrophil count delay below 0.5G /L for 7 days (Table 3).

Table 3. Analysis of risks to developing of pneumonia

Variable	Pneumonia occuring after chemotherapy (n=40)	No pneumonia after chemotherapy (n=98)	p	OR	95%CI
Age					
≥60	9	12	0.128		
<60	31	86			
Sex					
Female	25	42	**0.036**	**2.222**	**1.045-4.427**
Male	15	56			
AML	28	58	0.234		
ALL	12	40			
Response					

treatment					
Non- CR status	29	43	**0.002**	**3.372**	**1.514-7.509**
CR status	11	55			
Time period for neutrophils < 0.5 G/L					
≥ 7 days	26	38	**0.005**	**2.932**	**1.363-6.310**
< 7days	14	60			

Note: Non-CR status includcde not reached CR or previous not received chemotherapy

4. DISCUSSION

In our study, rate of pneumonia after chemotherapy was 29%, equivalent to the previous study [2], [3].

The symptoms of pneumonia in the group of pneumonia that occurs after chemotherapy tended to be milder than in the group of pneumonia that occurs before chemotherapy, reflected in the statistically significant lower frequency of dypsnea, respiratory failure, and degree of severity (with *P*=0.002, 0.004, 0.012; respectively). This result may be due to the lower average age, the lower rate of not having received specific chemotherapy before, and the higher rate of complete remission. These results indicate that chemotherapy to achieve complete remission can bring patients with acute leukemia to a more stable immune state, thereby reducing the severity of pneumonia. These results also help us to see that delayed treatment in patients with acute leukemia can lead to potentially more serious infections.

In our study, the female patient, complete remission status not ạchieved, a neutrophil count delay below 0.5G /L for 7 days, were risk factors for developing pneumonia after chemotherapy. The gender factor may affect the risk of developing pneumonia due to physical status. Chaoui D et al. also suggested that the performance status of the patients was an independent predictor of overall survival in patients with acute leukemia with pneumonia [7].

However, long-term neutropenia is generally accepted as a risk factor for infections, including pneumonia. Garcia JB et al. showed that neutropenia below 0.5 G/L was a risk factor in multivariate analysis [8]. Similarly, Specchia J et al. also indicated that long-term neutropenia was a risk factor [3]. Therefore, therapy should be considered to minimize the duration of neutropenia to reduce the risk of developing pneumonia.

The lack of complete remission is also a risk factor for the development of pneumonia. All Garcia JB, Specchia J, Wilhelm M suggested that the achievement of complete remission was an important prognostic factor for the recovery of pneumonia in patients with acute leukemia [3], [8], [9]. Thus, chemotherapy treatment aimed at achieving complete remission is an active measure to prevent complications of infection or pneumonia in the next chemotherapy sessions.

5. CONCLUSION

Pneumonia after chemotherapy for acute leukemia was common. Female patients, non-complete remission (CR) status (include: state of not reaching CR before or previous not received chemotherapy, a delay in neutrophil count below 0.5G /L for 7 days, were high- risk factors of developing pneumonia after chemotherapy.

Acknowledgment

We thank staffs of Center of Hematology and Blood Transfusion – Bach Mai Hospital.

REFERENCES

1. **Chandran R, Hakki M, Spurgeon S (2012).** Infections in Leukemia. Intechopen. Published: October 3rd, DOI: 10.5772/50193.
2. **Rossini F, Verga M, Pioltelli P, et al (2000).** Incidence and outcome of

pneumonia in patients with acute leukemia receiving first induction therapy with anthracycline-containing regimens. Haematologica. 85:1255–1260.

3. **Specchia G, Pastore D, Carluccio P, et al (2003).** Pneumonia in acute leukemia patients during induction therapy: experience in a single institution. Leuk Lymphoma. 44:97–101.
4. **Yoshida M, Akiyama N, Fujita H, et al (2011).** Analysis of bacteremia/fungemia and pneumonia accompanying acute myelogenous leukemia from 1987 to 2001 in the Japan Adult Leukemia Study Group. Int J Hematol. 93:66–73.
5. **American Thoracic Society; Infectious Diseases Society of America (2005).** Guidelines for the management of adults with hospital-acquired, ventilator-associated, and healthcare-associated pneumonia. Am J Respir Crit Care Med. 171:388–416
6. **Satici C, Demirkol MA, Altunok ES, et al (2020).** Performance of pneumonia severity index and CURB-65 in predicting 30-day mortality in patients with COVID-19**.** Int J Infect Dis. 98: 84–89.
7. **Chaoui D, Legrand O, Roche N, et al (2004).** Incidence and prognostic value of respiratory events in acute leukemia. Leukemia. 18:670–675.
8. **Garcia JB, Lei X, Wierda W, et al (2013).** Pneumonia during Remission Induction Chemotherapy in Patients with Acute Leukemia. Ann Am Thorac Soc. 10(5): 432–440.
9. **Wilhelm M, Kantarjian HM, O'Brien S, et al (1998).** Pneumonia during remission induction chemotherapy in patients with AML or MDS. Leukemia. 1996;10:1870–1873 factors. Chest. 114:444–451.

DEPRESSION AMONG STUDENTS AT THUYLOI UNIVERSITY

Le Cong Thien[1,2], Nguyen Van Tuan[1,2], Nguyen Thanh Long[1,2], Dao Ngoc Anh[1], Phung Tran Thu Hang[1], Pham Thi Hien[1], Vu Thi My Hanh[1], Cao Thi Anh Tuyet[2], Nguyen Dinh Trinh[3]

SUMMARY

Objective: *To characterize depression in students at ThuyLoi University.* ***Methods:*** *A cross-sectional study was conducted among students of ThuyLoi university.* ***Results:*** *Our study shows that depression by DASS 21 among the 2478 students, 14.2% of students participating in the interview experience major depression problems; 9.4% of students had moderate depression and 7.6% of students had mild depression. First year students, girl students, and students with childhood trauma have a higher percentage of having depression than other groups.* ***Conclusion:*** *Thus, through the results of practical research, we found that: the number of students with psychological problems, especially mild to very severe depression, accounts for nearly half of the students participating in the interview. This shows that this is a very urgent issue in universities in general and ThuyLoi University in particular. University should coordinate with medical facilities to regularly and timely advises students on psychological issues to improve the quality of students' health in the most comprehensive way.*

Key words: *depression, students, ThuyLoi university.*

1. INTRODUCTION

At the International Health Conference in New York (1948), the World Health Organization (WHO) defined health: “Health is a state of complete physical, mental and social well-being, rather than simply the absence of disease or infirmity” [1]. From there, it shows that mental health plays a very important role, on par with physical health and social health. Reality in today's society shows that lack of sleep, poor eating habits and lack of exercise are among the main causes of depression in college students. The stress that comes with a lot of pressures from around such as financial worries, pressure to get a good job after school and failed relationships can cause many students to leave college or be in bad shape.

According to a study conducted at Hai Phong Medical College by Nguyen Bich Ngoc and Nguyen Van Tuan, results were obtained. The study results showed that the stress rate of nursing students was 47.3% and stress level were 15.3%, 19%, 8.7%, 4.3% for mild, moderate, severe, and extremely severe respectively [2] According to research by Ahmed K. Ibrahim et al. in 2012, the depression rate among students in general ranges from 10% to 85%, of which the average rate is 30.6% [3]. In Vietnam, the prevalence of depression in school-age students is 4%-6% higher than in the general population, with the prevalence up to 16% [4]. In this age group, pressure from study and difficulties in life lead to boredom, disappointment, gradually giving rise to a feeling of pessimism and then leading to depression. Therefore, we have conducted this study to characterize depression in students at ThuyLoi University.

2. SUBJECTS AND METHOD

[1]Hanoi Medical University
[2]Mental Health Institute- Bach Mai Hospital
[3]ThuyLoi University
Corresponding author: Le Cong Thien
Email: vuhanh.psy44@gmail.com
Received date: 02/8/2022
Reviewed date: 15/8/2022
Accepted date: 15/9/2022

2.1. Study population and design

This cross-sectional was conducted through an online survey from April 22, 2022 to June 19, 2022 to assess depression characteristics among students at ThuyLoi University. There are a total of 2487 participants provided informed consent and conducted via Google form link.

2.2. Measurement

The questionnaire used in this study was built based on the DASS-21 (Depression Anxiety and Stress Scales) toolkit. DASS-21 is a rating scale developed by scientists from the University of New South Wales, Australia. DASS-21 can be used to screen for and assess levels of depression, anxiety and stress.

2.3. Data analysis

The research team used IBM SPSS Statistics 26 software to analyze the demographic characteristics, personal and family history of the participants, evaluate the level according to the DASS-21 scale and the correlation of the variables.

2.4. Research ethnics

The study was reviewed by the committee and approved by the leadership of the ThuyLoi university. This is a non-interventional descriptive study. Encrypted data to secured students information.

3. RESULTS

Tables 3.1. Demographic characteristics

Variables		n	%
Age		(Mean ± SD)	(20.19 ± 1.1)
	19	848	34.1
	20	706	28.4
	21	584	23.5
	22	328	13.2
	23 - 32	21	0.8
Gender	Male	1598	64.3
	Female	889	35.7
Student year	First-year	909	36.6
	Second-year	697	28.0
	Third-year	574	23.1
	Fourth-year	307	12.3
Current residence	Live with family	764	30.7
	Live in lodging	1282	51.5
	Live in the dormitory	429	17.2
	Other	12	0.5
The family lives in	Area 1	204	8.2
	Area 2	1128	45.4
	Area 2 – countryside	584	23.5
	Area 3	571	23.0

Among 2487 study participants, the proportion of 19-year-old participants accounted for the most 34.1%, followed by 20-year-old participants accounted for 28.4% and 21-year-old participants accounted for 23.5%. The 22-year-old group accounted for 13.2% and the 23-32-year-old group accounted for at least 0.8%. The average age group participating in the study was 20.19 ± 1.1. The proportion of male participants (1598 persons) in the study was 1.8 times higher than that of female participants (889 persons).

Table 3.1 shows that the percentage of first-year students is 36.6%, followed by second-year students with 28.0% and 23.1% of third-year students. Fourth-year students account for the lowest percentage is 12.3%. Most of the participants lived in lodging, accounting for 51.5%. Participants living with their families accounted for 30.7% and 17.2% participants living in dormitory. According to the results, the majority of study participants live in area 2, accounting for 45.4%. Participants live in area 3 (23.5%) and area 2 – countryside (23.0%) with similar proportions. Area 1 accounts for at least 8.2%.

Table 3.2. Personal history

Variables	n	%
Childhood traumas:		
Yes	46	1.8
No	2441	98.2
Total	2487	100.0

Table 3.2 shows that the majority of participants did not experience childhood trauma, accounting for 98.2%. However, a small number of participants experienced childhood trauma, accounting for 1.8%.

Table 3.3. Family history

Variables		n	%
Family members with mental illness	Yes	15	0.6
	No	2472	99.4
Parent's relationship	Harmony	2300	92.5
	Conflict	44	1.8
	Separation/ divorce/ illness/ death	143	5.7

According to the research results, there were 15 participants, equivalent to 0.6% of people with family members suffering from mental illnesses and 99.4% of families of study participants without mental illnesses. Most of the participants' parents' relationships were harmonious, accounting for 92.5%. 5.7% separated/ divorced/ illness/ dead and 1.8% of participants had parents in conflict.

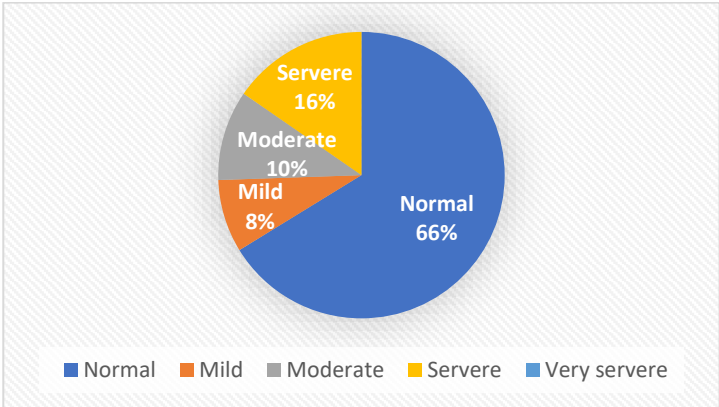

Figure 1. Percentage level of depression

There are 14.2% of students participating in the interview experience major depression problems; 9.4% of students had moderate depression and

7.6% of students had mild depression. Most of the students who participated in the interviews were normal, did not have depression problems (61.2%), the remaining 7.6% of the students had very severe depression.

Table 3.4. Distribution between depression and socio-demographic characteristics (n=2487)

Variables	None n (%)	Depression n (%)
Gender:		
Male	1063 (66.5)	535 (33.5)
Female	459 (51.6)	430 (48.4)
Age		
19-20 years old	945 (60.8)	609 (39.2)
21-22 years old	565 (62)	347 (38.0)
23-24 years old	11 (57.9)	8 (42.1)
>= 25 years old	1 (50)	1 (50)
Education level		
First year	540 (59.4)	369 (40.6)
Second year	435 (62.4)	262 (37.6)
Third year	353 (61.5)	221 (38.5)
Fourth year	194 (63.2)	113 (36.8)
Childhood trauma		
No	1509 (61.8)	932 (38.2)
Yes	13 (28.3)	33 (71.7)

Females were higher than males in having depression for those without depression where males (66.5%) were slightly upper than females (51.6%). About >=25 years old students were superior (50%) in having depression compared to other age categories. In regards to educational level, a first year level was the most depressive among the other year levels. Out of 46 people with childhood trauma, the number of students with depressive problems accounted for 71.7%.

4. DISCUSSION

Anxiety and depression are common problems in the field of psychiatry. These disorders can occur at any age, especially in recent years, the disease tends to increase due to many aspects of socio-economic impacts. These disorders have an incidence of 3-5% of the population, often arise at a young age, are more common in women than in men, can lead to serious consequences such as the risk of suicide.

According to our research, students have a very severe depression level of 7.6% (188 students out of 2487 students participated in the interview).

As Kevin WC Lun's study indicated, among the 1119 valid questionnaires analyzed, 767 (68.5%) were found to have mild to severe depressive symptoms. In which, students have severe depression from 1.4%-3.2% [5].

Josephine GWS Wong and colleagues conducted the study showing that a total of 7915 students completed the survey, with a response rate of 27.5%. The average level of depression was 21% [6]

And our research shows that 9.4% and 14.2% are the respective percentages of students with moderate and severe depression.

Normal and mild depression levels of students at ThuyLoi University are 61.2% and 7.6%, respectively, as shown in our study.

We compared with the research paper of Thai Nguyen University of Medicine and Pharmacy, we find that the results of the study are quite similar, that study also shows that female gender, first year students and stress are factors associated with higher rates of depression [7].

This shows that mental health, especially depression, has a significant impact on university students in general and students at ThuyLoi University in particular.

5. CONCLUSION

There are 14.2% of students participating in the interview experience major depression problems; 9.4% of students had moderate depression and 7.6% of students had mild depression. Most of the students who participated in the interviews were normal, did not have depression problems (61.2%), the remaining 7.6% of the students had very severe depression. Female gender, first year students and stress are factors associated with higher rates of depression.

Thus, through the results of practical research, we found that: the number of students with psychological problems, especially mild to very severe depression, accounts for nearly half of the students participating in the interview. This shows that this is a very urgent issue in universities in general and Thuy Loi University in particular. Universities should coordinate with medical facilities to regularly and timely advises students on psychological issues to improve the quality of students' health in the most comprehensive way.

Acknowledgment

We thank students at ThuyLoi University for participating this study.

REFERENCES

1. Constitution of the World Health Organization. <https://www.who.int/about/governance/constitution>, accessed: 08/23/2022.
2. **Ngọc N.B. and Tuấn N.V. (2021).** Thực trạng stress của sinh viên điều dưỡng Trường Cao đẳng Y tế Hải Phòng năm 2020. TCNCYH, 143(7), 159–166.
3. **Ibrahim A.K., Kelly S.J., Adams C.E., et al. (2013).** A systematic review of studies of depression prevalence in university students. Journal of Psychiatric Research, 47(3), 391–400.
4. **Trang L.N.B., Trâm Đ.T.N., and Cường Đ. (2017).** A study on depression and some relevant depression risk factors among high school and university students in Da Nang city. UD-JST, 20–22.
5. **Lun K.W., Chan C.K., Ip P.K., et al. (2018).** Depression and anxiety among university students in Hong Kong. Hong Kong Med J, 24(5), 466–472.
6. **Wong J.G.W.S., Cheung E.P.T., Chan K.K.C., et al. (2006).** Web-based survey of depression, anxiety and stress in first-year tertiary education students in Hong Kong. Aust N Z J Psychiatry, 40(9), 777–782.
7. **Hoa D.T.B., Luu L.T., Vinh N.D. (2022).** Thực trạng và một số yếu tố liên quan đến lo âu, trầm cảm ở sinh viên ngành y khoa Trường Đại học Y Dược Thái Nguyên. Hội Thần Kinh Học Việt Nam.